



HAL
open science

Microseismic activity and fluid fault interactions: some results from the Corinth Rift Laboratory (CRL), Greece

Seid Bourouis, François Henri Cornet

► To cite this version:

Seid Bourouis, François Henri Cornet. Microseismic activity and fluid fault interactions: some results from the Corinth Rift Laboratory (CRL), Greece. *Geophysical Journal International*, 2009, 10.1111/j.1365-246X.2009.04148 . hal-01385700

HAL Id: hal-01385700

<https://hal.science/hal-01385700>

Submitted on 21 Oct 2016

HAL is a multi-disciplinary open access archive for the deposit and dissemination of scientific research documents, whether they are published or not. The documents may come from teaching and research institutions in France or abroad, or from public or private research centers.

L'archive ouverte pluridisciplinaire **HAL**, est destinée au dépôt et à la diffusion de documents scientifiques de niveau recherche, publiés ou non, émanant des établissements d'enseignement et de recherche français ou étrangers, des laboratoires publics ou privés.

Microseismic activity and fluid fault interactions: some results from the Corinth Rift Laboratory (CRL), Greece

S. Bourouis¹ and F. H. Cornet²

¹Centre de Recherche en Astronomie, Astrophysique et Géophysique; Route de l'observatoire, 16006 Bouzareah, Algérie

²Institut de Physique du Globe de Strasbourg-CNRS, 5 rue René-Descartes, 67084 Strasbourg, France. E-mail: francois.cornet@eost.u-strasbg.fr

Accepted 2009 February 17. Received 2009 February 17; in original form 2008 May 18

SUMMARY

The Gulf of Corinth, in western-central Greece, is one of the fastest continental rifts in the world. In its western section near the city of Aigion, the previous work has outlined the existence of a shallow dipping seismogenic zone between 5 and 12 km. This seismic activity has been monitored with a network of 12 three-component stations for the period 2000–2007. Three, few months long, seismic swarms have been observed. They mobilize a complex structural fault system that associates both shallow dipping elements and subvertical structures with very different azimuths, some of which extend to depths greater than that of the shallow dipping zone. The swarm activity associates intensely active, short crises (a few days) with more quiescent periods. The long-term growth velocity of the seismically activated domains is compatible with a fluid diffusion process. Its characteristics are discussed in the context of the results from the 1000 m deep AIG10 well that intersects the Aigion Fault at 760 m. The vertical growth directions of the seismically activated volumes outline two different sources for the fluid and imply non-steady pressure conditions within the seismic domain. The diffusivity along the cataclastic zone of the faults is in the order of $1 \text{ m}^2 \text{ s}^{-1}$, while faults act as hydraulic barrier in the direction perpendicular to their strike. If the vertical direction is a principal stress component, the high pore pressure values that must be reached to induce slip on the shallowly dipping planes can result only from transitory dynamic conditions. It is argued that the shallow dipping active seismic zone is only local and does not correspond to a 100 km scale decollement zone. We propose to associate the localization process with deep fluid fluxes that have progressively modified the local stress field and may be the cause for the quiescence of the West Heliki Fault presently observed.

Key words: Permeability and porosity; Fault zone rheology; Seismicity and tectonics; Back-arc basin processes; Dynamics and mechanics of faulting.

1 INTRODUCTION

The Gulf of Corinth, in western-central Greece, is one of the most seismically active zones in Europe (e.g. Makropoulos 1989; Hatzfeld *et al.* 2000; Burton *et al.* 2004). A compilation of the cumulated seismically radiated energy for Greece (magnitudes larger than 2.5), as computed from the National Observatory of Athens catalogue for the 1970–2007 period (NOA 2007), is shown in Fig. 1(a). On this map the Corinth Rift is clearly outlined. However, a closer analysis shows that the seismicity in the western part of the rift is very different from that in the eastern part, as shown in Fig. 1b, which outlines the number of recorded events rather than the cumulated radiated energy. In the western part near Aigion, the microseismicity is characterized by very frequent earthquake swarms (generally with magnitudes smaller than 4.5) that last a few months, whereas much more energetic (magnitudes close to 7),

but much less frequent seismic events, occur in the eastern section (Alchimedea Peninsula, AP in Fig. 1b).

Near the city of Aigion (Aig in Fig. 1b), some 40 km East of Patras (in Fig. 1b), previous investigations conducted with temporary seismic networks (Rigo *et al.* 1996; Gautier *et al.* 2006) have outlined a 3–4 km thick seismically active zone. It is shallowly dipping (about 20°) to the north from a 5–8 km depth range at the south shore to a 9–12 km depth range near the northern shore. The 1995 magnitude 6.2 earthquake that occurred north of Aigion at a depth close to 10 km (Bernard *et al.* 1997) mobilized a shallow dipping fault zone (about 30° dip).

But the 1981 seismic sequence (three earthquakes with magnitude ranging from 6.3 to 6.7), which occurred near the Alchimedea Peninsula, mobilized faults with dips ranging from 50 to 60° (Hubert *et al.* 1996). To the west, in the Trichonis Basin (TB in Fig. 1b), the seismic crisis that occurred in April 2007 (Kiritzi

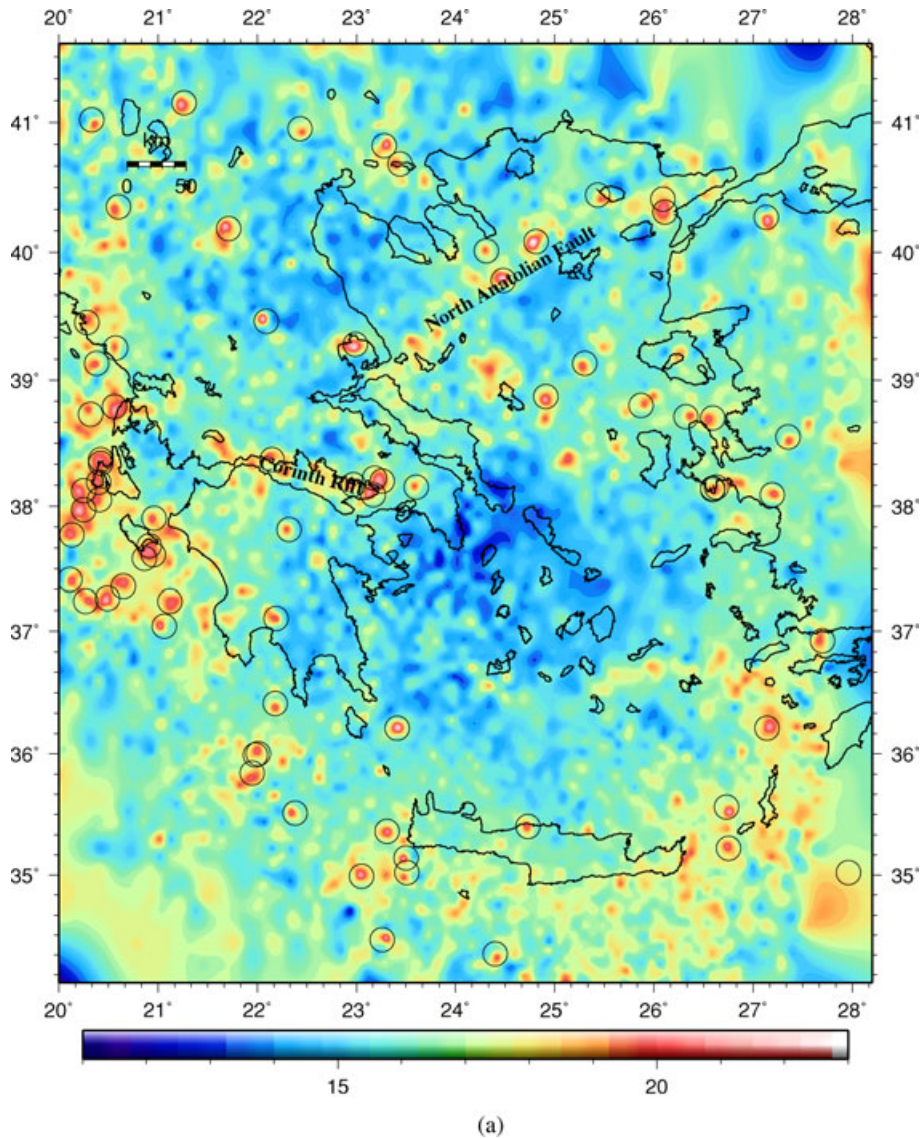


Figure 1. (a) Map of cumulated seismically released energy for the 1970–2007 period as determined from the NOA catalogue; pixels are $8 \text{ km} \times 8 \text{ km}$. For this compilation the local M_1 magnitudes of the catalogue have been converted to M_s magnitudes according to the Burton *et al.* (2004) relationship (their eq. (11c)) and then M_s magnitudes have been converted to seismically radiated energy according to the Kanamori & Anderson (1975) empirical equation (17) in which energy is expressed in dyne cm. The colour scale is logarithmic so that the numbers correspond to 10^{15} and 10^{20} erg (dyne cm) ($1 \text{ erg} = 10^{-7}$ joules).

et al. 2008) includes two $M_1 > 5$ earthquakes with dip on planes oriented, respectively, N317°E and N325°E and dipping 65° and 67° to the north. It involves events that occurred down to depths close to 20 km. Hence, the shallow dipping seismic zone remains fairly constrained near Aigion within the rift.

Yearly GPS campaigns have been repeated over 11 yr (Avalone *et al.* 2004) and help to characterize the regional deformation process. They are consistent with an extension rate in the N185° E direction, which is equal to about 11 mm yr^{-1} in the central part of the rift (Xilocastró), but which reaches 16 mm yr^{-1} in the western section near Aigion.

For the western part of the rift, outcropping faults exhibit at ground surface dips to the north in the 60° range and questions have been raised on the relationship between the shallow dipping seismogenic zone and the steeply dipping outcropping faults. It has often been proposed (Briole *et al.* 2000; Bernard *et al.* 2006) that

the outcropping normal faults do not change dip with depth but stop on a so-called detachment zone located at the base of the shallow dipping seismic volume, the displacement characteristics of which have been adjusted to be consistent with GPS data.

However, both high resolution seismic reflection and multibeam bathymetric data, collected offshore slightly east of Aigion, have outlined the existence of South dipping normal faults close to the northern shore (McNeil *et al.* 2005; Bell *et al.* 2008).

Since 1999, a multidisciplinary observatory known as the Corinth Rift laboratory (CRL) has been developed in the Aigion area. The objective is to investigate *in situ* the mechanics of active faults and more specifically their quasi-static and dynamic interactions, with special emphasis on the role of fluids (e.g. Cornet *et al.* 2004). This *in situ* laboratory includes, among other sensors, a network of 12 three-component (2 Hz) seismic stations (CRLnet), a set of five continuous GPS stations together with a Sacks–Evertson borehole

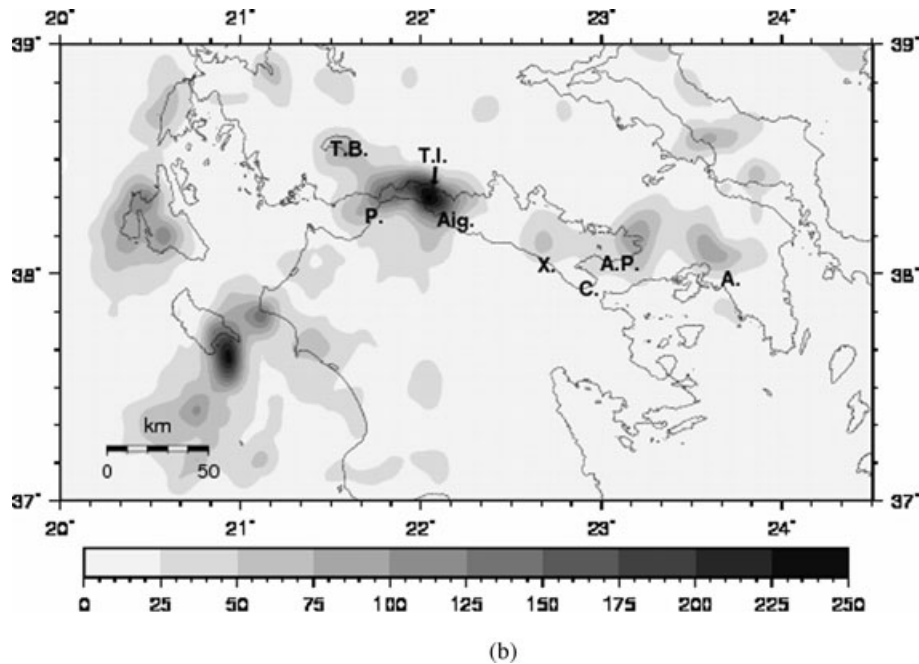


Figure 1. (Continued.) Total number of events per unit area (8 km \times 8 km) for the period 1970–2007 (after NOA catalogue) P is Patras, Aig is Aigion, X is Xylocastro, C is Corinth, AP is the Alchimedies Peninsula, A is Athens, TI is the Trizonia Island and TB is the Trichonis Basin.

dilatometer and a long base tiltmeter (Bernard *et al.* 2007), as well as the 1000 m deep instrumented AIG10 well that intersects the Aigion Fault around 760 m.

We discuss in this paper results from 8 yr of microseismic monitoring at CRL, taking into account some observations conducted in the AIG10 well. This 8-yr continuous seismic monitoring outlines three main crises. The first one, in 2001, has already been described elsewhere (Lyon-Caen *et al.* 2004; Pacchiani & Lyon-Caen 2009), and we analyse first the growth pattern of the 2003–2004 and 2006–2007 crises.

Then we examine the relationship between steeply outcropping normal faults and the observed shallow dipping seismogenic zone and finally discuss, for the three seismic swarms, the possible role of fluid diffusion and the related question of the fluids sources.

2 MICROSEISMIC ACTIVITY OBSERVED WITH CRLnet FOR THE 2000–2007 PERIOD

The daily seismic activity recorded by CRLnet ranges from 10 to 20 events per day during periods of quiescence, with magnitudes M_1 generally smaller than 2. However, this activity may reach up to 150 events per day during seismic crises. In 2005, this continuous activity has prompted us to adopt automatic picking procedures for arrival times reading and automatic location determination for a monthly follow-up of the local activity.

The automatic detection procedure concerns both P and S phases. The P phase detection combines algorithms proposed by Baer & Kradolfer (1987) and by Earle & Shearer (1994). It is based on the comparison between short-term average (STA) and long-term average (LTA) signal characterization. The picking of S phases follows Cichowicz (1993) procedure and exploits the three signal components for identifying S phases from their polarization diagram. Efficiency of the method has been validated by comparing results from ‘manual’ picks and from ‘automatic’ picks. The sample involves

659 events. Differences in phase picking were better than 0.1 s for more than 70 per cent of the events. Further, only 3.2 per cent of the signals were not identified by the automatic picking procedure.

Location determination has been run with the 1-D velocity model adopted by Rigo *et al.* (1996). It involves a minimum of $5P$ and $3S$ arrival times and rms smaller than or equal to 0.2 s. Differences in horizontal locations between manual and automatic picking are smaller than 2 km for 75 per cent of events and smaller than 1 km for 60 per cent of them. Because S picking is slightly less accurate than the picking of P phases, differences in depth determinations are smaller than 2 km for only 50 per cent of the events.

Some 30 000 events with magnitudes larger than 0.5 have been identified and located for the 8-yr observation period. They are shown in Fig. 2 together with the location of seismic stations and of the 1000 m deep AIG10 well.

To explore the variation of seismic activity with time, we have defined three volumes (3-aa’, 3-bb’, 3-cc’) that are shown in Fig. 2. These volumes extend perpendicularly to the horizontal reference plane down to 30 km. For each domain, we plot in Fig. 3, the horizontal distance between hypocentres and a vertical plane (shown as the line passing through letters a, b and c, in Fig. 2) serves as a common arbitrary reference for all events.

Fig. 3-aa’ clearly illustrates the lack of activity on the southern shore of the rift, except for the 2001 crisis that lasted about 4 months. Fig. 3-bb’ shows that another two main crises have occurred during the 8-yr observation period, namely the 2003 October–2004 June crisis and the 2006 September–2007 May crisis. In addition, a more or less diffuse activity is continuously observed throughout the duration of observation. Fig. 3-cc’ helps to characterize the development in time of the 2006–2007 crisis in the northern shore of the rift. It also shows that no additional major crisis occurred below the northern shore of the rift over this 8 yr period.

Both major swarms identified in Fig. 3b exhibit a somewhat similar characteristic, namely we identify slow moving fronts over

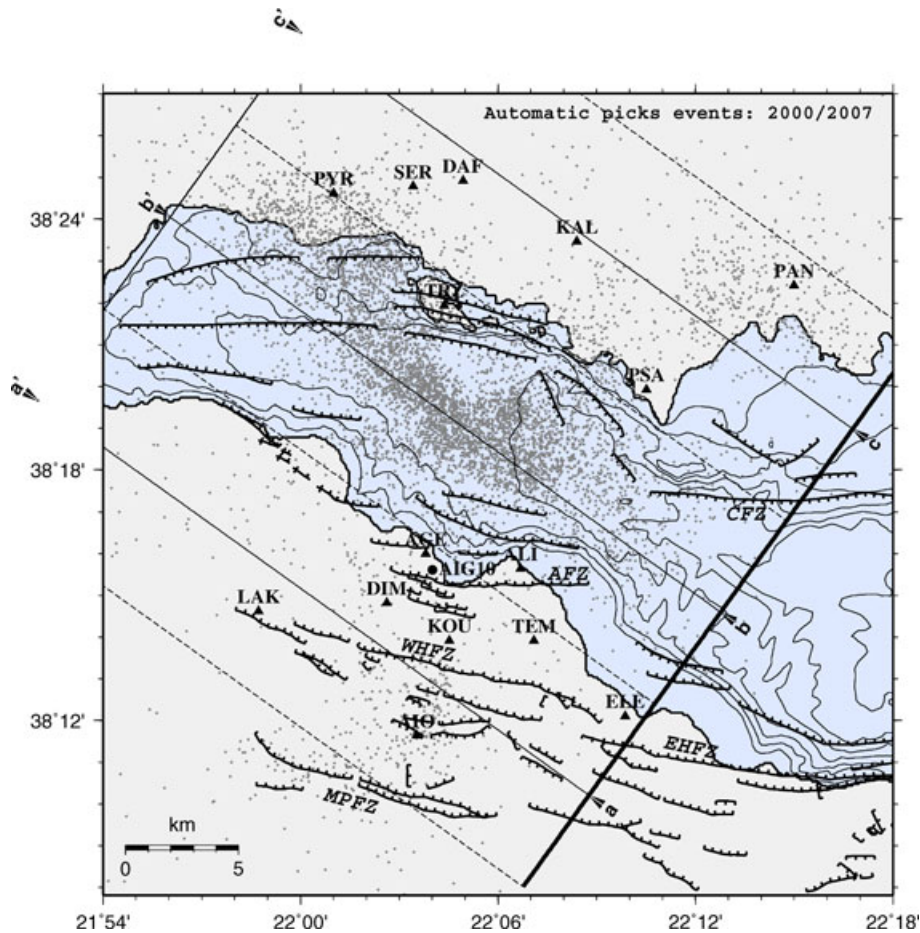


Figure 2. Map of events for the 2000–2007 period as determined with CRLnet, with location of stations and indication of vertical subvolumes presented in Fig. 3; results from automatic event detection procedure. AIG10 is the location of the 1000 m deep AIG10 well. MPFZ is the Mamoussia Pyrgaki Fault zone, WHFZ and EHFZ are, respectively, the West and East Heliki Fault zones, AFZ is the Aigion Fault zone, CFZ is the Channel Fault zone. The thick line passing through points a, b and c is the surface trace of the vertical plane taken as reference for evaluating horizontal distances in Fig. 3 (see the text).

the entire crisis duration and the occurrence of short-lived (a few days to a few weeks) crises with a very high density of events during fairly restricted periods. This microseismic activity is somewhat reminiscent of the swarm activity described by Hainzl & Fischer (2002) in the Eger Rift, in the Vogtland/NW Bohemia area (see also Hainzl & Ogata 2005). These authors conclude that the spatial development of the swarm activity cannot be explained by a simple fluid diffusion process. Instead they propose a relationship between spatial spreading and moment release that they relate to the slip mechanism. However, they consider an initial intrusion of fluid as the likely origin of the swarm activity. But this same Eger Rift swarm has also been analysed by Parotidis *et al.* (2003) who conclude to the good fit between the spatial growth of the swarm and a mechanism of fluid percolation. In the next two sections, we analyse the growth of the swarm activity for both the 2003–2004 and the 2006–2007 microseismic crises to explore whether fluid diffusion may be operating in the Aigion area.

Before the automatic event location determination procedure was developed, arrival times were picked manually (Lyon-Caen *et al.* 2004). These readings were based on the CRLnet data but were often complemented by readings from neighbouring networks. These included PSLnet to the west, which is managed by the Seismological Laboratory from Patras University, Cornet and Atnet to the east,

which are managed by the University of Athens. In addition, a temporary seismic tomography experiment has been run with close to 80 stations during 9 months in 2002 (Gautier *et al.* 2006).

For this data set (period 2000–2004) event location involves a minimum of 5*P* and 4*S* arrival times and rms smaller than or equal to 0.1 s, so that location resolution is better than 1 km on all components. About 12000 events have been manually picked for this period (a few months have been left out when little activity was observed according to the automatic detection procedure). Epicentres location is indicated in Fig. 4. It outlines very clearly the 2001 crisis that occurred on the south shore. Further, it exhibits clusters that outline local structures. We note that cluster I appears as subvertical structures with a south-oriented dip direction on the cross-sections shown in Fig. 5 (vertical projection 5-dd'). In this figure, the cross-section 5-cc' outlines a steeply dipping active zone that extends below 10 km, under the shallow dipping seismic zone. Finally, on this same 5-cc' cross-section, events as deep as 13 km are observed below the cloud generated by the 2001 crisis.

These data show that the shallow dipping seismogenic zone north of Aigion, as described in the literature, does not correspond to a single planar structure. It includes numerous steeply dipping zones with both north and south dips, but their vertical extension remains to be ascertained. Thus, the shallow dipping slip plane as identified

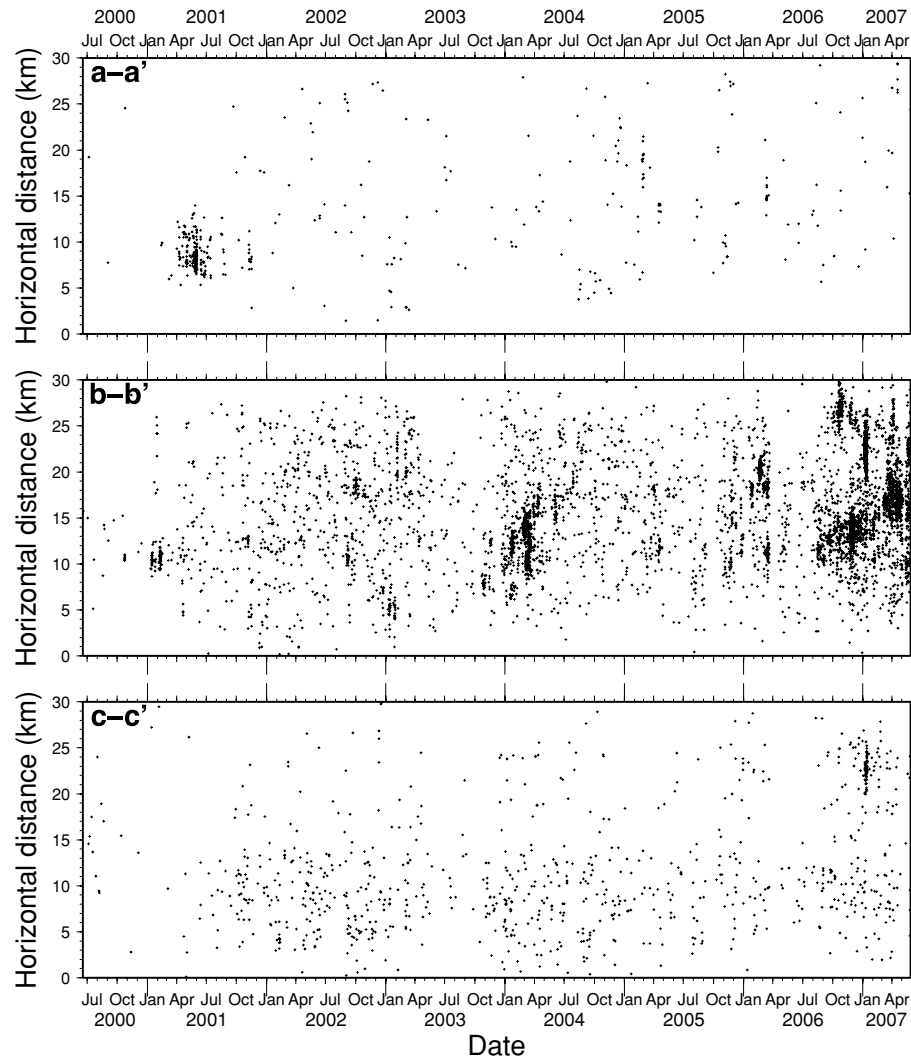


Figure 3. Change of distance of events with time, for the three subvolumes defined in Fig. 2. Origin is the arbitrary vertical plane marked by a thick line passing through points a, b and c in Fig. 2.

from multiplet analysis in this region (Rietbrock *et al.* 1996) must be viewed as only one of the slip surfaces that control the mechanics of this domain.

2.1 The November 2003–June 2004 microseismic crisis

Here we consider only event locations based on manually picked arrival times so that location accuracy is within 1 km for all components. In Fig. 6 we explore the development of the crisis and plot with respect to time the distance r between events observed at time t and the barycentre of the initial cluster of events that occurred on 2003 October 24. It outlines the coexistence of light, diffuse seismicity observed continuously all over the observation area and local microseismically active zones characterized by short-lived outbursts of activity within a slower, longer term growing process. The general tendency is for a linear increase of the distance between the furthest away events and the initial cluster barycentre with time, with a mean growth velocity equal to about 2.3 m hr^{-1} .

Four main clusters in time (A, B, C and D) have been identified in Fig. 6. The location of events from these clusters is shown in Figs 7a and b. Fig. 7b illustrates the vertical growth of this activity.

Initially in Fig. 7c, a downward migration is observed from 5 to 7 km whereas on the long term the mean growth occurs within the 7–9 km depth range. Fig. 7b also shows event magnitudes as determined from signal duration; they range between 1 and 3.

To obtain a clearer picture of the corresponding structures we have adopted the three-point technique that Fehler *et al.* (1987) developed for analysing microseismic activity induced during hydraulic stimulation for geothermal energy exploitation. The method is based on the observation that microseismic activity induced by large-scale fluid injections in crystalline rocks is generated by shear along more or less planar structures. However, the lack of resolution for events' locations yields a somewhat blurred image of the planar structures. The method runs in two steps. First it determines for all possible combinations of three events the plane that passes through the corresponding three events. Then it identifies the most often picked dip and strike values.

Fehler *et al.* propose a technique for correcting for the shape of the seismic cloud to identify substructures within the seismic cloud. We have not adopted this corrective technique here, given that the objective of the analysis is indeed to detect the characteristic geometrical shape of the seismic cloud and not to identify its substructures. The three-point technique as applied here

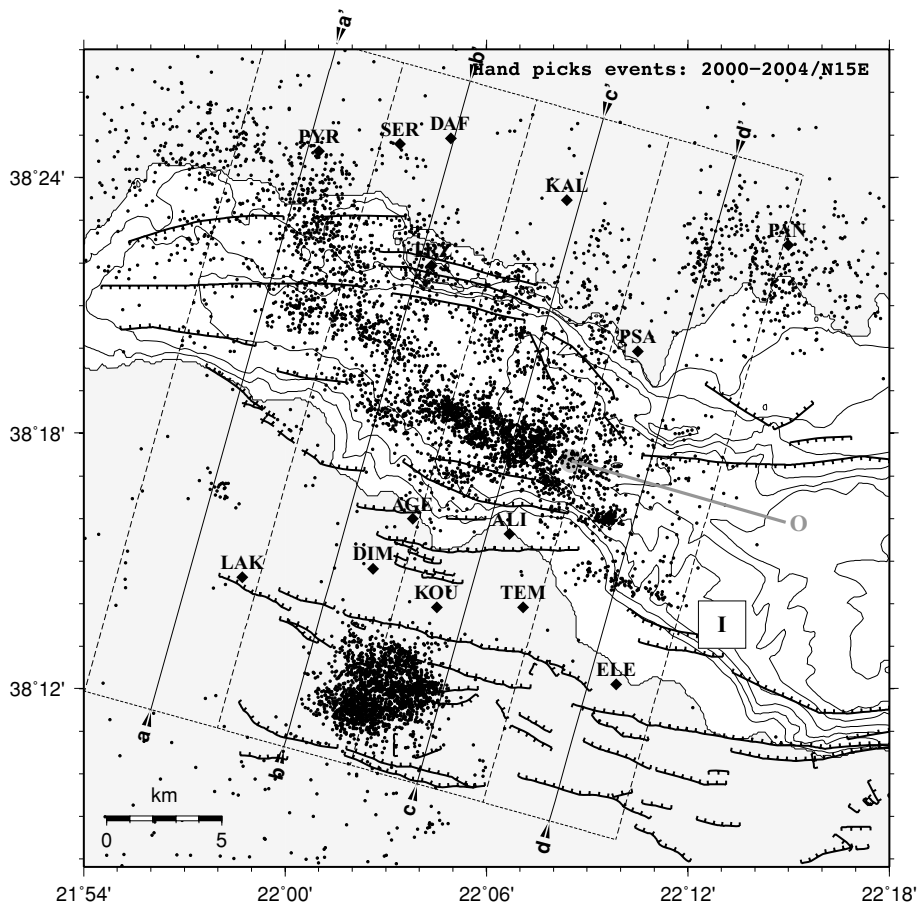


Figure 4. Location of hand-picked events for the 2000–2004 period, with indication of echelon I, mentioned in the text. Horizontal projection of subvolumes (aa' , bb' , cc') oriented $N15^\circ E$ discussed in Fig. 5 are indicated. O is barycentre of events for 24 October 2003.

does not look for a best fitting plane; it only identifies a mean direction for the seismic cloud without any consideration on the ‘thickness’ of the cloud in the direction perpendicular to this mean direction.

In Figs 8a–d we consider successively time clusters A–D of Fig. 6. They outline a complex structure. For cluster A, a rather well-defined south dipping planar structure is identified. However, as seen on the horizontal projection 7a, events are mostly clustered close to the barycentre with some occasional events occurring at a large distance from the barycentre. These far away events are most likely not associated directly with the structure activated during this swarm but correspond to the regular diffuse seismicity pattern observed all over the 8 yr of observation. Further, from a purely statistical perspective, this uneven spatial distribution of events invalidates the three-point technique that assumes a rather uniform coverage of the cloud under investigation. So this result is not considered as reliable. For cluster B, the three-point method identifies a main direction subparallel to the rift direction (strike orientation of the structure is $N106^\circ$ that is subvertical (3° with respect to vertical direction). This event geometrical distribution is also compatible with substructures of similar direction but with different dip values, ranging from $N50^\circ$ to $N90^\circ$ and from $S45^\circ$ to $S90^\circ$. Clusters C and D also involve geometries parallel to the rift orientation but with very variable dip. The most often picked dip is subhorizontal for these two clusters, outlining the largest horizontal extension of the cloud as compared to its vertical extension. However the southern dip of the pole is somewhat different to the north shallow dipping

geometry previously described during short-term (a few months) observation periods (Rigo *et al.* 1996; Gautier *et al.* 2006) and also seen in Fig. 5.

These results suggest that the shallow dipping seismic zone that has been often assimilated to a decollement zone involves in fact substructures with very different orientations many of which are steeply dipping. They also outline that the deformation of this zone involves processes that occur at different timescales. Cluster B of events that outlines a simple subvertical planar structure occurs over about a 1-month period through successive short-lived (a few days) crisis. However, the whole crisis lasts about 6 months with a progressive growth from east to west over a distance close to 10 km. Finally, a somewhat en-echelon structure visible in Fig. 4 appears only when considering all the events over a 4-yr-long period.

It may be pointed out that no acceleration in the displacement field across the rift, as monitored with the continuous GPS stations, is noticeable during the corresponding time period (rms on daily variations for monthly periods are ranging from 6 to 8 mm according to P. Briole—www.corinth-rift-lab.org). Further, no transitory signal is detected in the borehole dilatometer installed on Trizonia Island, some 8 km north of Aigion (resolution better than 10^{-7} per year, Bernard *et al.* 2006). This provides an upper bound to the size of the slip displacement that has occurred during the various short-lived crises. It may also result from the effects of the regional geological structure. Indeed, previous to the rift activity, the Tertiary Alpine tectonics generated numerous nappes with the most superficial one (the Pindos Nappe) made up of a highly folded and faulted stack of

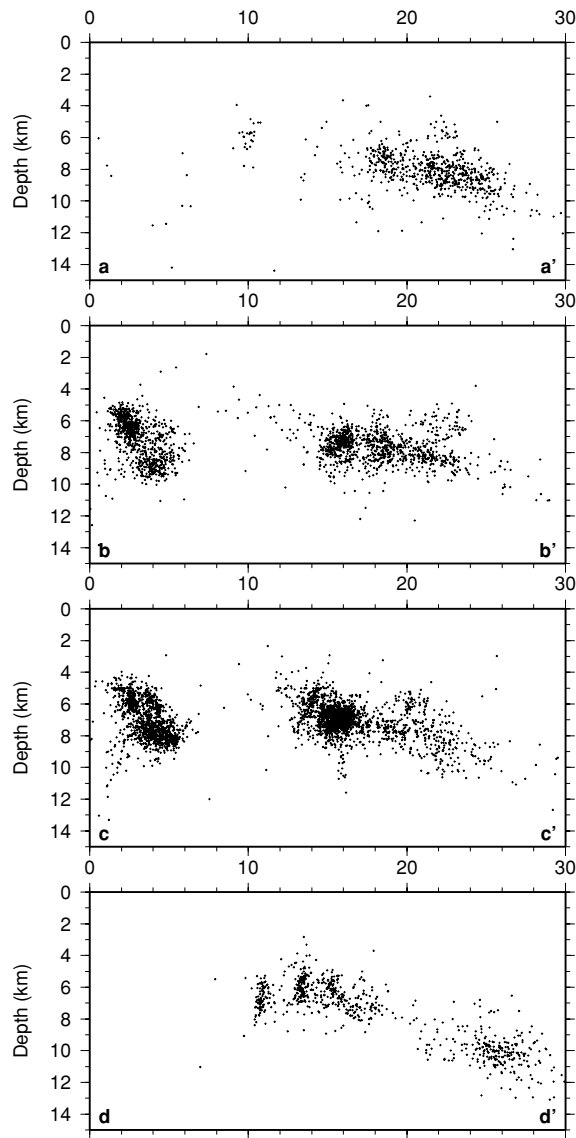


Figure 5. Vertical projections of hypocentres in the four domains indicated in Fig. 4. Orientation of the volumes is $N15^\circ E$. Note that the cross-section cc' includes events at depths in the 8–12 km depth range, on the south shore (see the text for discussion). Note the South dipping structures in section dd' .

radiolarite clay interbedded with thin limestone beds (Jolivet *et al.* 2004). Such a material clearly exhibits a non-elastic behaviour on the long term, as shown by results from the AIG10 well (see discussion in Section 3.2), which poses difficulty to associate small fault displacements at depth with observed ground surface displacement fields.

These observations show that the deformation process involves different timescales and structures that are not simply structurally related to one another (i.e. they do not constitute a simple roughly overall planar structure), contrary to what has been described for the growth of single fault systems (e.g. Main 1996; Hainzl & Fisher 2002). We propose here, as a simple phenomenological interpretative model, a fluid diffusion process within a complex structure that involves both subvertical and shallow dipping structural elements that are close to static equilibrium. When pore pressure increases slightly, it increases the effective Coulomb shear stress so that local

failure conditions are reached. The slow (2 m hr^{-1}) growth process would correspond to the diffusion process whereas the short-lived crisis would correspond to fault instability resulting, possibly, with increased fluid diffusivity as discussed later. Given the slow downward growth direction of the seismic cloud, if a diffusion process is the cause of the observed seismicity, then the downward migration implies a superficial source of fluid for this crisis. Further, the more than 10 km horizontal extension as compared with the less than 5 km downward extension must be addressed. If fluid diffusion is a significant component of the observed activity, then this observation will be consistent with a significant decrease in fluid diffusivity below 8–9 km, in the centre of the gulf, or with a less critical regional effective stress field.

This simple interpretative model, that reconciles the large extension of the seismic cloud with the absence of detectable deformation detected at ground surface, will be further discussed after the 2006–2007 seismic crisis has been examined.

2.2 The September 2006–May 2007 seismic crisis

For this crisis only automatic event detection is available so that uncertainties on depth determinations are smaller than or equal to 2 km. We plot in Fig. 9 the horizontal projection of the monthly activity from 2006 January to 2007 May. It shows a major seismic crisis starting sometime during 2006 August, to the southeast of Trizonia Island (TI on Fig. 1b). The barycentre of all events observed during August within the squared shaded area shown in Fig. 9(h) is chosen as the spatial origin O1 of the seismic crisis (also shown in Fig. 11).

The geographical growth of this patchy activity is presented in Fig. 10. When all events are plotted simultaneously, a more than 25 km long complex structure becomes visible with two subparallel branches grossly oriented $N135^\circ E$, separated by a domain oriented grossly in the $N70^\circ E$ direction. Interestingly this $N70^\circ$ oriented structure is mostly active from August to December 2006 and becomes nearly non-seismic thereafter, when the activity becomes mostly localized along the $N135^\circ$ oriented branches. It is located just north of the domain that was activated by the 2003–2004 crisis. In Fig. 11 we plot for the period 2006 August–2007 May the distance between event hypocentres and the barycentre of events observed during 2006 August versus the time that elapsed between the corresponding event occurrence and 2006 August 14. The mean growth velocities are in the same order as those evaluated for the 2003–2004 crisis growth, namely from 1 to 4 m hr^{-1} . However, contrary to the 2003–2004 crisis that outlines a single growing domain, the 2006–2007 crisis shows two originally independent sources of activity that migrate towards each other. The second source of activity starts in 2006 October, close to point O2 identified in Figs 9J and 11.

To obtain a clearer picture of the vertical extension of these structures we have plotted for the same periods event depth distributions with azimuth (Fig. 12a–c). Most events occur in the 6–9 km depth range. However, as time passes, the proportion of events located at depth greater than 9 km increases to the northwest of point O2 (with some events located below 12 km). In addition, for the last period (from days 180 to 300), an upward growth is noticed in the $N120^\circ E$ direction (with some events close to 3 km). In Fig. 13 we plot the seismic activity within vertical slices about 6 km wide and oriented $N60^\circ E$. These figures outline two subparallel structures in section bb' . Their orientation is estimated to be close to the $N30^\circ W$ direction, from an analysis of similar plots drawn in

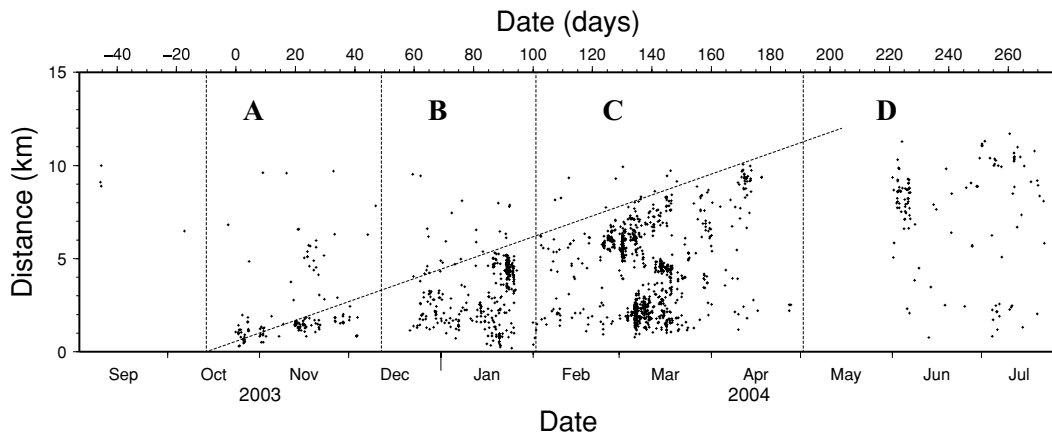


Figure 6. Variation of distance (vertical axis) with time (horizontal axis) for the 2003–2004 crisis. The origin for the distance evaluation for the event locations is the barycentre of events observed on 24 October 2003. The straight line shown in the figure is only used for an approximate evaluation of the mean velocity of the motion of the pressure front (see the discussion in Section 3).

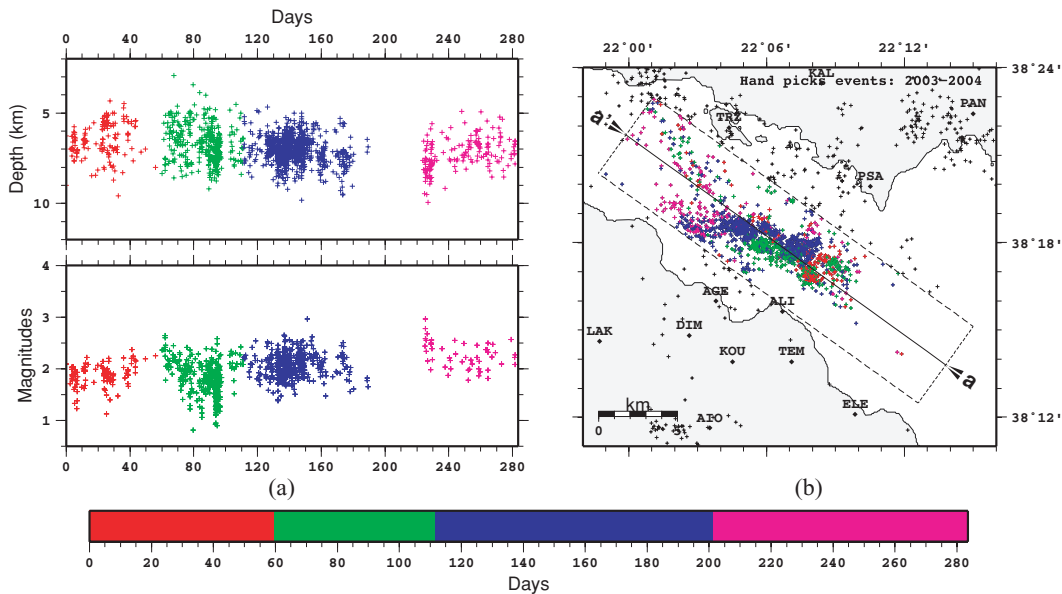


Figure 7. (a) Right: hypocentre locations for events of the four clusters A (red), B (green), C (blue) and D (pink) identified in Fig. 6. (b) Left: depths of hypocentres for clusters A, B, C and D and corresponding magnitudes evaluated from signal duration. Time origin is 24 October. (c) Variation of hypocentre depth distribution over 40-day periods. Note the initial downward growth during the first 80 days.

azimuths ranging from 0 to 90°, at 5° increments. This direction is close to that identified in Fig. 10, for the two main branches of the seismic cloud. Yet no structure of similar orientation has been described in the regional geology; they correspond likely to structures that developed prior to the Alpine tectonic structures. This implies that the local 3–4 km thick nappe regional structure strongly overprints the ground-surface displacement field generated by motion along these deep structures and creates strong difficulties for monitoring with surface sensors the deep displacements below the nappe.

As for the 2003–2004 crisis, the 2006–2007 seismic crisis involves deformation processes with different time characteristics. We can identify repeated short-lived (few days) crises and long-duration (multimonths) deformation processes. However, for the 2006–2007 crisis, the activated structure is more complex than that activated in 2003–2004. Further it involves two simultaneous cen-

tres of activity that seem to interact progressively. Considerations on depth extension of the activity show that the activity starts within the 6–9 km range, with both upward and downward extension near the end of the crisis (2007 February–May).

At the monthly timescale, this seismic activity does not seem to be simply linked to an external source of fluid that diffuses uniformly either upwardly or downwardly, throughout the whole activated structure. Instead, results suggest that the source of pressure is generated by the deformation process itself. The slip associated with the short-lived crisis generates stress variations that in turn induce changes in fluid pressure. However simultaneously, the short-lived crises modify the hydraulic properties of activated zones, depending on the amount of slip and the associated dilatancy. Its modelling requires a precise understanding of the location, geometry and amount of slip for the various small-scale failed zones (few days long seismic crises). It would also require some knowledge of the

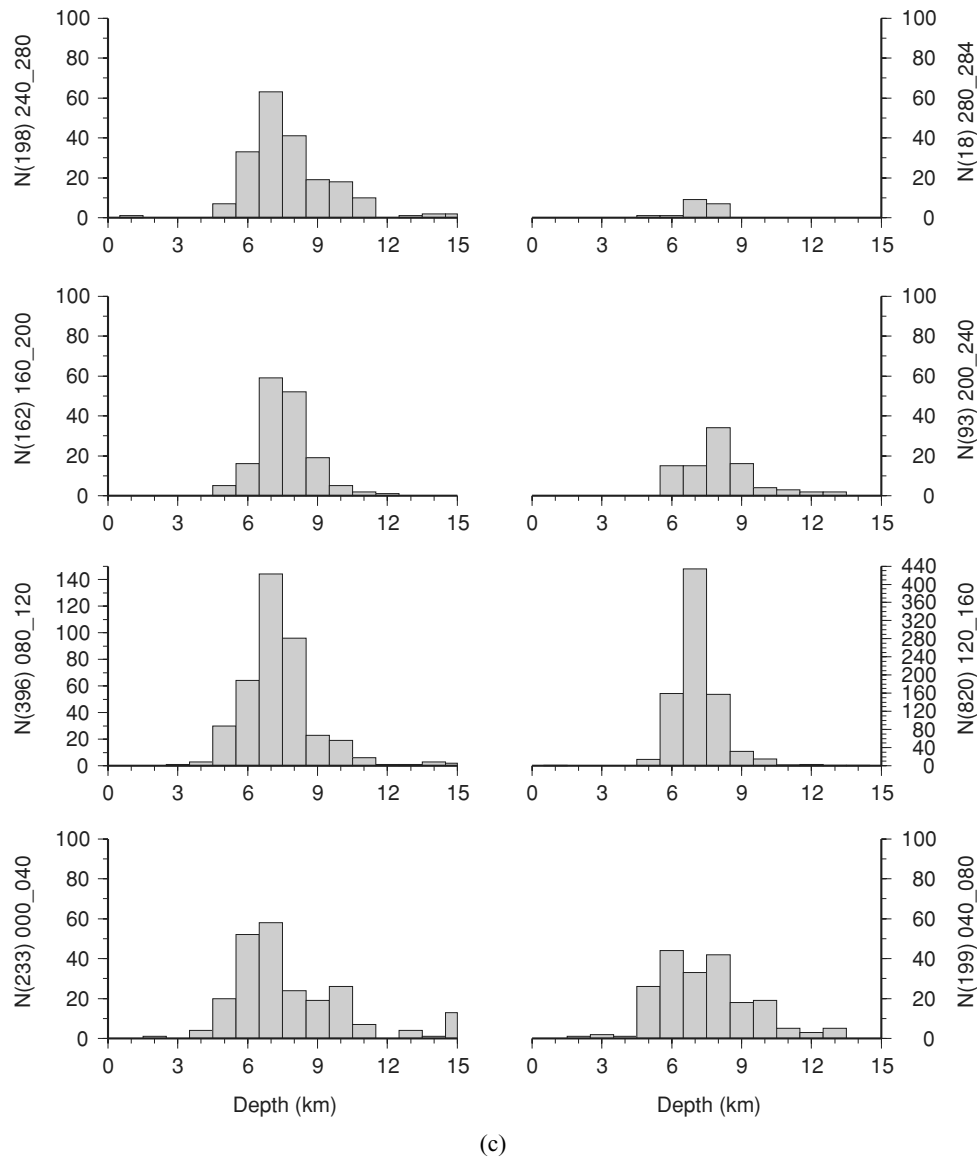


Figure 7. (Continued.)

initial local hydraulic permeability and of the storage capacity of the geomaterial (continuum equivalent to the combination of rock matrix, fault and fracture pattern, fault and fracture filling) involved by the deformation process. It will be undertaken only after complementary geophysical reconnaissance provides the required constraints on main structural elements.

3 ON THE ROLE OF FLUIDS IN AIGION'S AREA SEISMIC CRISES

Both the 2003–2004 and 2006–2007 seismic crises outline two different timescales in the deformation process and we have proposed to associate the short-lived crises mostly with slip along pre-existing structures and the long-term behaviour with fluid diffusion. We examine further now the hypothesis on the role of fluid diffusion for the long-term component of seismic swarms at CRL by comparisons with induced seismicity observed in geothermal exploitation and during dam impoundment, as well as by comparison with seismic swarms observed in the Eger Rift zone.

3.1 Is fluid diffusion a significant component for the swarm activity at CRL?

Many examples of microseismic activity generated by anthropic pore pressure increase have been described in the literature. They concern the filling of dam reservoirs (Bell & Nur 1978; Gupta 1983; Talwani & Acree 1984; Simpson *et al.* 1988) or the injection of fluids at depth (Healy *et al.* 1968; Pearson 1981; Cornet & Yin 1995; Shapiro *et al.* 1997; Cornet *et al.* 2007).

The seismicity induced by reservoir impoundment has been linked to both, the load increase brought by the mass of water in the reservoir and the pore pressure increase because of fluid diffusion. To separate both mechanisms, reference is made to the timing of the processes as well as to the distance between the location of the event and the reservoir location, with the load increase effect being synchronous to the reservoir water level increase.

Two hypotheses are formulated for investigating the relationship between microseismicity and fluid diffusion. It is assumed that the seismic signal is generated by a shear event triggered by an increase in pore pressure and that the growth of the microseismic cloud is

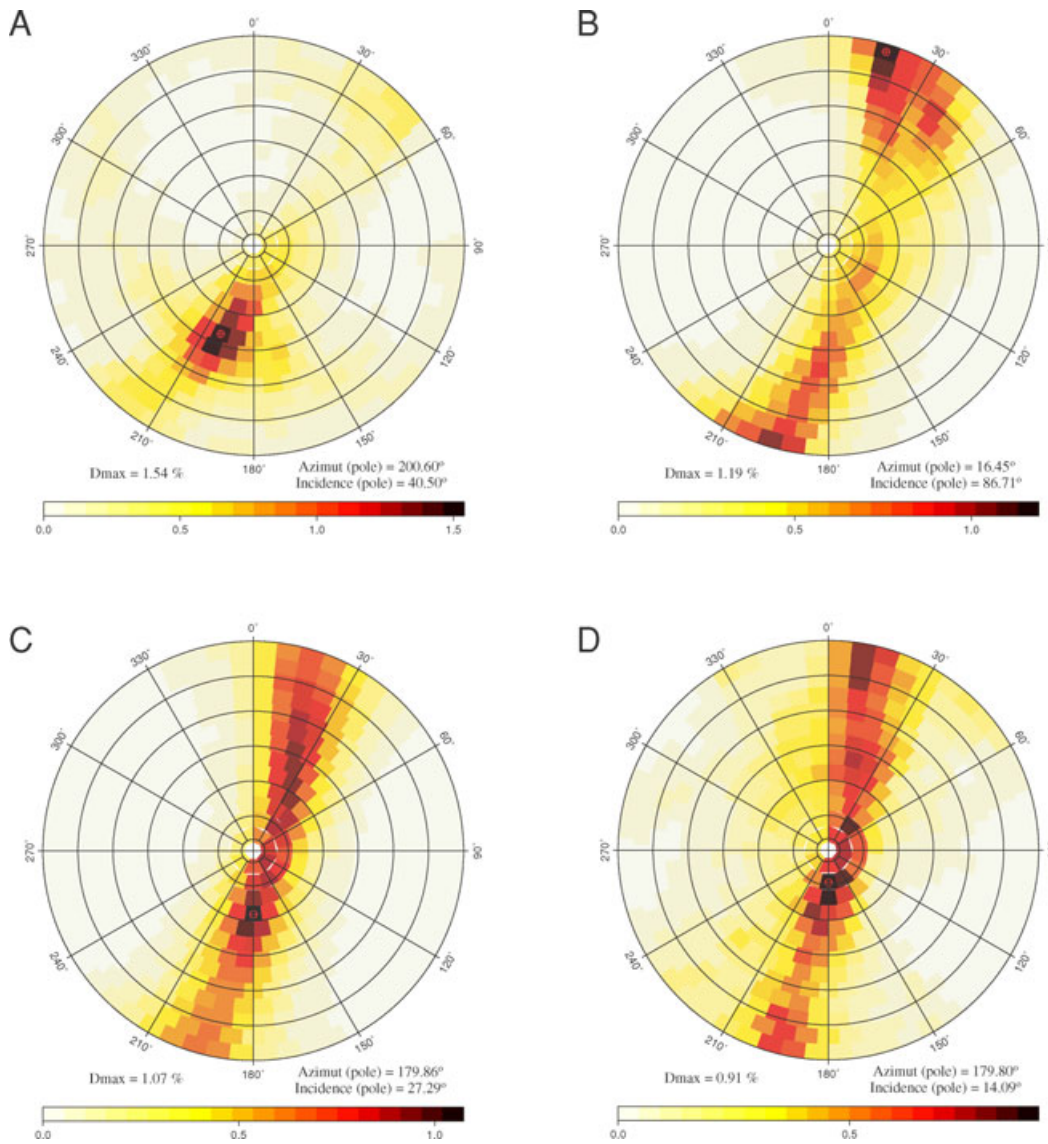


Figure 8. Identification of poles for the main cloud orientation of clusters. A, B, C and D correspond to periods defined in Fig. 6. The radial value is the pole incidence (angle of normal to plane with respect to the vertical direction). It varies from zero (horizontal planes) at the centre of the diagrams to 90° (vertical plane). The colour code indicates the percentage of the total number of solution investigated. The pole identification in (a) is not considered meaningful because of uneven spatial events distribution (see Figs 6 and 7a and the text). Period B outlines a main fault zone in the N106° E direction and a secondary fault direction N140° E somewhat similar to that identified during the 2006–2007 swarm.

associated with the migration of the pressure front in an unperturbed domain. This supposes that shear motion along a seismically activated structure does not affect its hydraulic conductivity. Each individual seismic slip is assumed to be small enough so as not to influence the equivalent continuum material property. With such a model Talwani & Acree (1984) were the first to outline a linear increase of the growth of the area with time where epicentres appear around dams. Assuming that the fluid source is controlled by the water level in the dam, they proposed to relate this linear relationship to a fluid diffusion effect and obtain orders of magnitude for the rock mass diffusivity (that depends on both the rock mass permeability and the rock mass storage coefficient) in the 5×10^3 – $6 \times 10^5 \text{ cm}^2 \text{ s}^{-1}$ range, for domains extending down to depths in the order of a few kilometres below the reservoir.

Shapiro *et al.* (1997) have examined many examples of seismicity triggered by fluid injections in boreholes and considered the rate of

growth of the microseismic cloud, away from the well as a means to evaluate the rock mass diffusivity. Assuming that it is independent of pore pressure and the microseismic activity, they describe the fluid diffusion by the uncoupled equation (1)

$$\partial P / \partial t = D \nabla^2 P, \quad (1)$$

where P is the pore pressure and D is the rock mass diffusivity. They solve eq. (1) for a step-function pressure point source in a homogeneous isotropic medium and estimate the distance r at time t of the propagating front of a given pore pressure perturbation chosen large enough for triggering a local unstable slip (front of over pressure value in the 1 MPa range). The solution is given by

$$r = \sqrt{4\pi Dt}. \quad (2)$$

By assimilating the location of seismic events the furthest away from the injection point with the location of the pressure front at time t ,

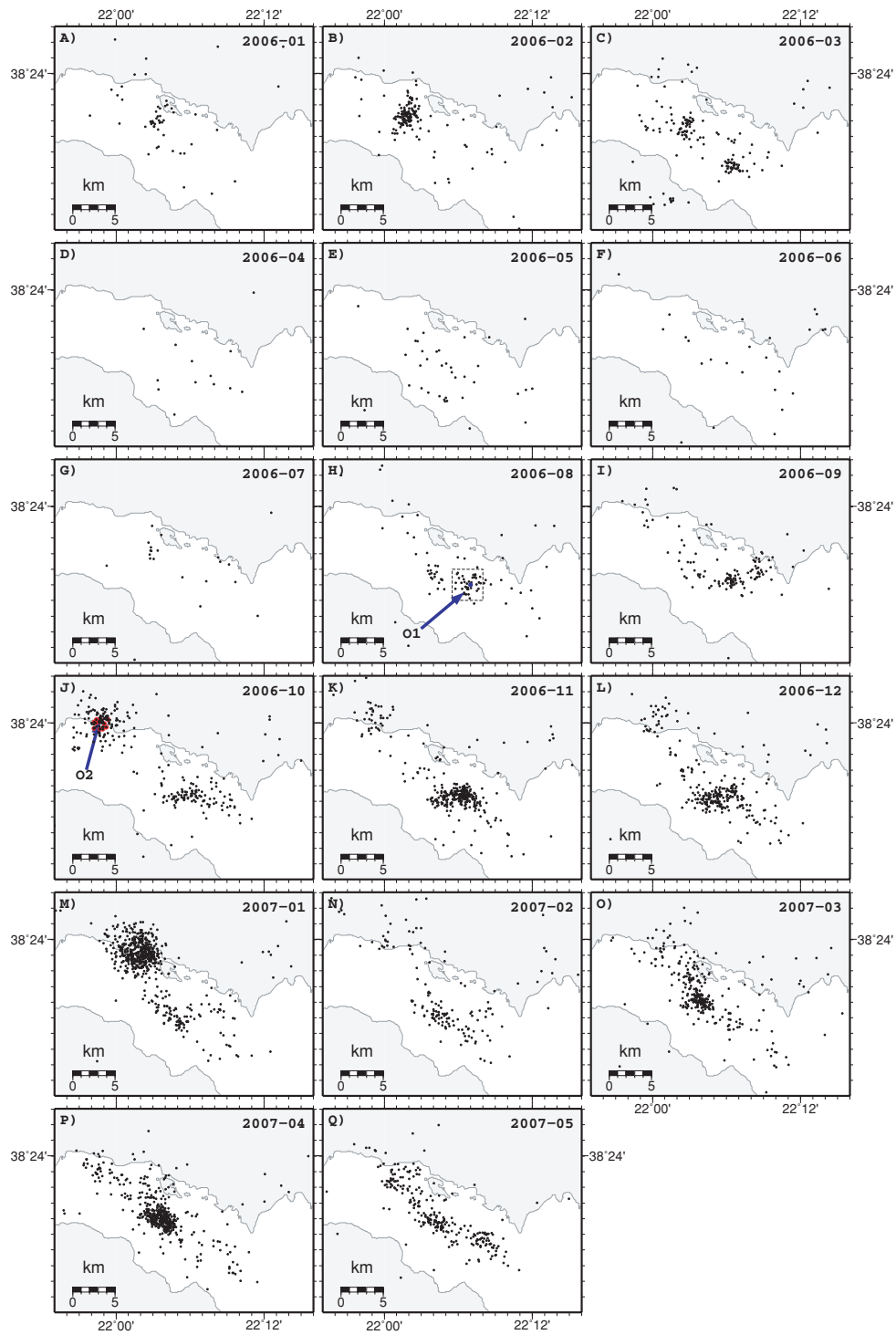


Figure 9. Horizontal projection of monthly activity for the January 2006–July 2007 seismic swarm. The barycentre of events observed in August 2006 has been selected as origin for the plots shown in Figs 10 and 12. Point O2 taken as reference for the origin of the second centre of activity identified in October 2007 (Figs 3 and 11, and discussion in the text) is also shown.

they obtain an estimate of the rock mass diffusivity. For this purpose they plot, for all events, the distance between the corresponding event and the fluid source with respect to time. The parabola adjusted to fit the envelope of the plot yields an estimate of the rock mass diffusivity. With such a model, they come up with diffusivity values in the 0.5×10^4 – 2×10^4 $\text{cm}^2 \text{ s}^{-1}$ range for an injection run around the 8 km depth in the KTB borehole, in eastern Germany, close to

the Eger Rift already mentioned. However, as pointed out by Cornet (2000), this modelling remains valid as long as the water injection does not induce any large-scale failure process in the rock mass that would affect its hydraulic diffusivity, in other words as long as fluid diffusion may be modelled by the uncoupled equation (1).

Parotidis *et al.* (2003) have applied Shapiro *et al.*'s parabola fitting approach to the swarm that occurred from August to December

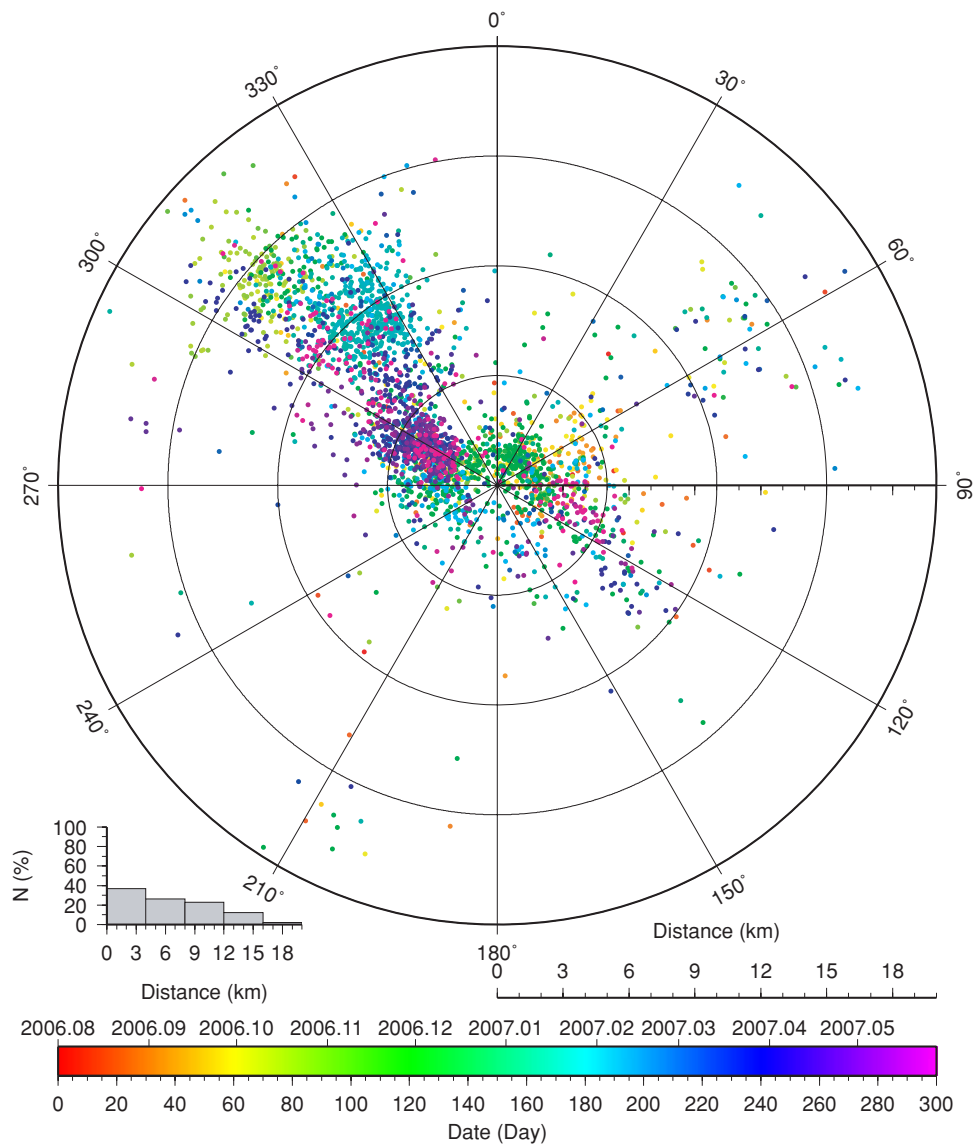


Figure 10. Azimuthal variation with time (colour code) of distances between epicentres of events of the 2006–2007 swarm with respect to barycentre 01 of epicentres observed in August 2006. The figure outlines two subparallel structural directions with a N135° E orientation somewhat reminiscent of the direction identified during period B of the 2003–2004 swarm activity.

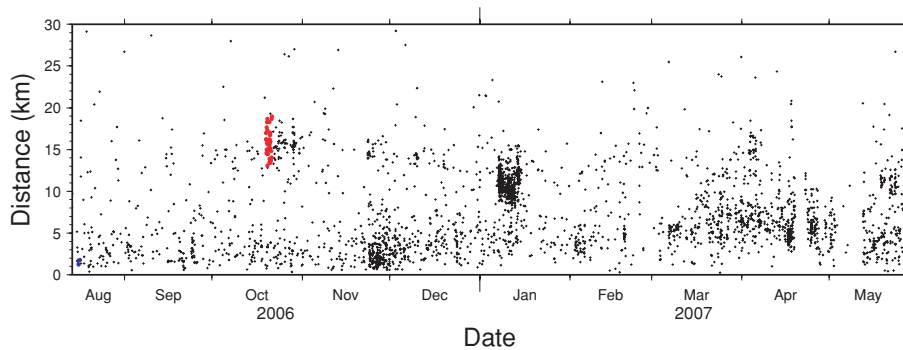


Figure 11. Analysis of the 2006–2007 swarm development with time. We plot versus time (horizontal axis) the distance between event hypocentres and the barycentre of events observed during August 2006 (vertical axis.) Events considered for identifying the origin O2 of the second centre of seismic activity are shown in red

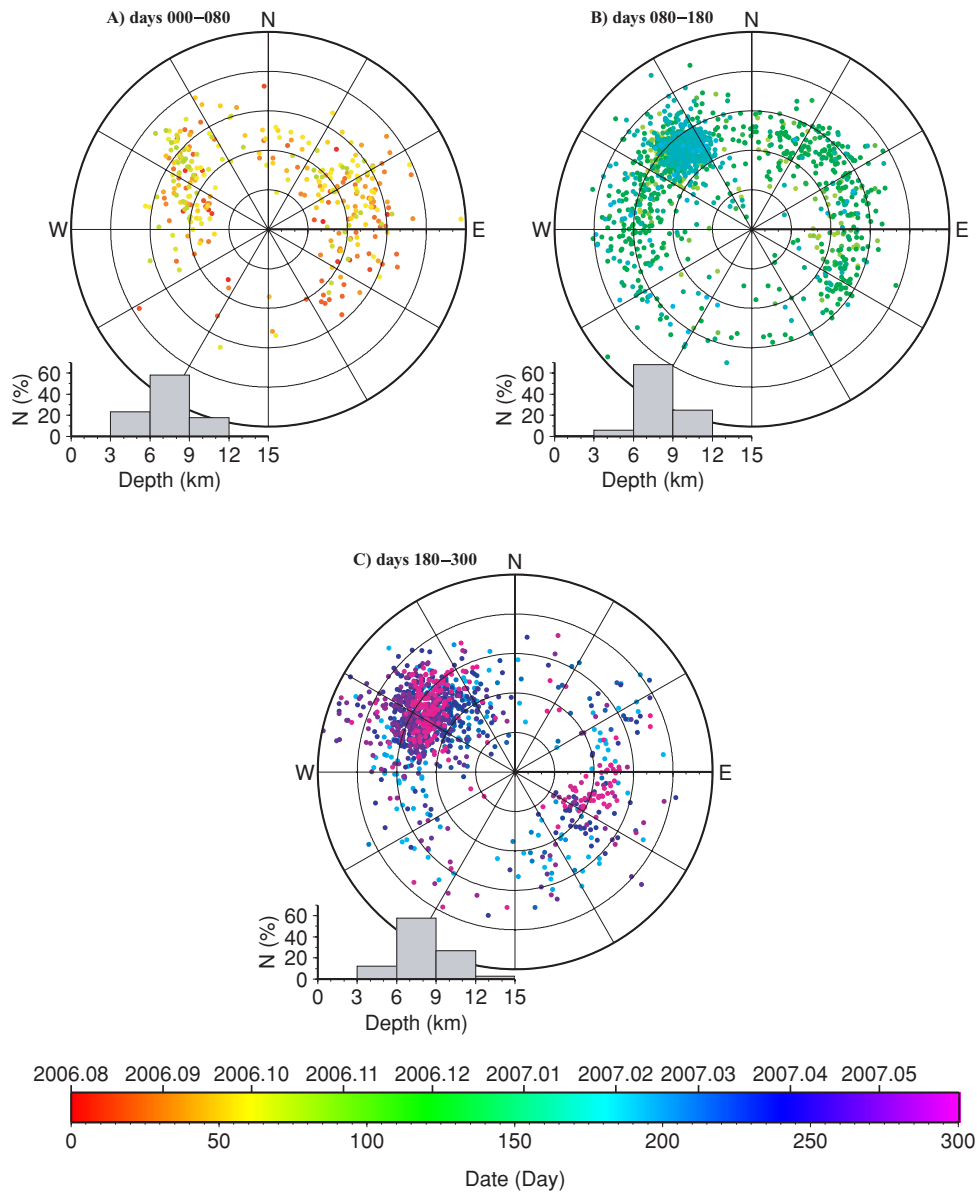


Figure 12. Azimuthal variation of depth with time (colour code) for three time periods (12A: days 0–80; 12B: days 80–180; 12C: days 180–300). A downward migration in the northwest zone and an upward migration in the South East domain are noticeable at the end of the swarm activity.

2000, in the Eger Rift region. As pointed out by Hainzl & Fisher (2002), as well as by Parotidis *et al.*, there is a convergence of observation pointing towards a strong role of fluids of magmatic origin in this swarm activity. Interestingly, as for the Corinth Rift swarms, two different timescales are apparent: periods of strong activity that last a few days separated by periods of quiescence resulting in an overall slow growth of the seismically active zone. For the 2000 Eger Rift swarm, a very clear overall upward growth is observed through nine main activity periods. Parotidis *et al.* have modelled this swarm development by a fluid diffusion process assuming a step-function fluid point source. Thus, they adopt the parabola fitting procedure for determining the hydraulic diffusivity from the growth of the seismic cloud generated by each cluster of activity without any consideration on the coupling between the fluid diffusivity characteristics of faults and the fault shear behaviour. They come up with diffusivity values ranging from 0.3×10^4 to $10 \times 10^4 \text{ cm}^2 \text{ s}^{-1}$. However, Hainzl and Fisher have concluded that,

although fluids play an active role in the initial swarm activity, the growth process for each individual cluster of activity is controlled by stress redistribution rather than by fluid diffusion. However Hainzl and Fisher's analysis does not address the long-term component of the swarm activity, that is the multiday quiescence periods between main activity phases.

Clearly, the step-function point-source model considered by Parotidis *et al.* for the fluid source in natural deformation processes is likely not exact and the uncoupled flow equation is over-simplistic. Yet this simple model provides a useful appraisal for orders of magnitude for the growth rate of seismicity to be expected from fluid diffusion. With this respect we note that values observed at CRL are very similar to those observed at the Eger Rift.

From these strong similarities, together with similarity in growth rate values observed in both natural swarms and man-made fluid induced seismic clouds, but also because the overall structure of the seismically activated zone is generally not quite planar, we conclude

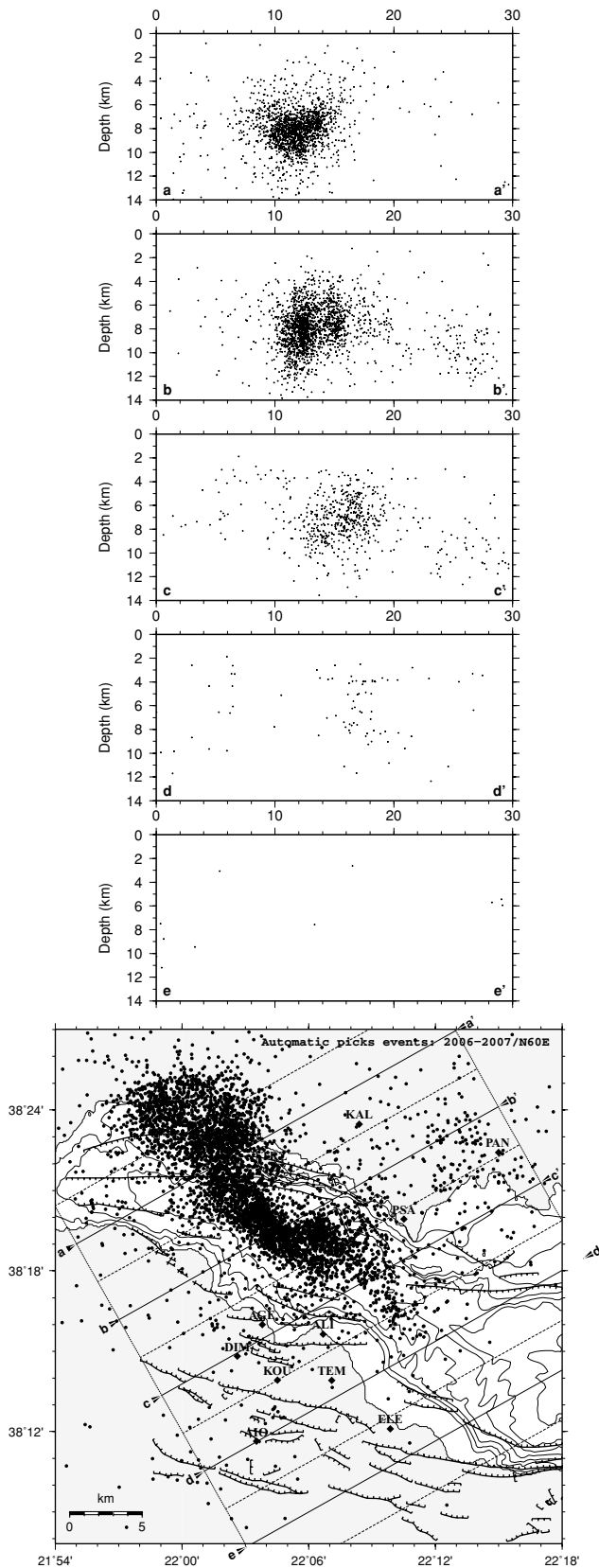


Figure 13. Location of events determined automatically during the 2006–2007 swarm activity. (a) Horizontal projection showing the orientation of the vertical subvolume described in (b). (b) Vertical projection of events in vertical subvolumes about 6 km wide and oriented N60° E. Note the two structures in section bb' (see the text).

that the long-term activity for swarms at CRL is very consistent with a fluid diffusion model. We explore next these diffusion processes for the three main seismic crises that have occurred during the 2000–2007 period in the Aigion area.

3.2 Possible sources of fluids

3.2.1 The 2003–2004 seismic swarms and the AIG10 well observations

The 2003–2004 swarms started at CRL about 1 month after some strong hydraulic disturbances occurred in the 1000 m deep AIG10 well in Aigion. This well intersects the Aigion Fault around 760 m and was meant in part to provide an *in situ* characterization of its morphology and of its hydromechanical properties (Cornet *et al.* 2004b; Daniel *et al.* 2004; Sulem *et al.* 2004; Song *et al.* 2004).

Cuttings and core analysis together with vertical seismic profiles have shown that the fault dip is about 60° down to 800 m and that the fault has supported a total vertical offset in the order of 200 m (Place *et al.* 2007). The fault itself is about 8 m thick, with two hydraulically conductive cataclastic zones separated by an inner 0.5 m thick argillaceous core. The fault has been shown (Giurgea *et al.* 2004) to constitute a hydraulic barrier between an upper aquifer (0.5 MPa overpressure above hydrostatic) and a lower aquifer (1.0 MPa overpressure above hydrostatic). The upper aquifer in platy limestone from the Pindos Nappe is overlaid by a 300 m thick impervious formation that involves about 100 m of quaternary subhorizontal clays overlying a heavily tectonized cretaceous series of radiolarites and platy limestone (Fig. 14). The lower aquifer is developed in a heavily karstified carbonate formation of the Gavrovo-Tripolitza nappe (Rettenmeier *et al.* 2004). The fault core itself is made of an impervious 0.5 m thick impervious clay zone surrounded by somewhat permeable cataclastic zones. Results from the temperature profiles indicate that convection occurs within the karstified limestone below the fault (Doan & Cornet 2007a). The regional heat flux, as evaluated from the temperature profile above the fault, is equal to 53 mW m⁻². It implies a temperature in the 160–170°C range around 8 km.

On 2003 September 24, the well was let produce water over its entire uncased length (from 711 m down to 1000 m) and then was closed at the well head. During this production, the flow rate reached values in the order of 250 m³ hr⁻¹ over periods reaching a few hours. When the well was closed, it was filled with water over its entire length so that, upon closing the well, the pressure of the lower karstic aquifer was applied over the entire openhole section of the well.

A simple hypothesis is that the increase of pore pressure in the aquifer above the fault has induced some slip along the fault that resulted in a break of Aigion Fault seal between aquifers at greater depth. Consequently, the water from the fossil karst has progressively diffused within the cataclastic zone in the hanging wall of the fault. No significant upward diffusion is possible, given the thick argillaceous cover. Further, the diffusion process has generated seismic activity only once it reached depths where the conditions for seismic slip were satisfied, and not at shallower depths where quasi-static creep may dominate.

Hence, we propose that the 2003–2004 seismic crisis is related to this fault motion. With this simple hypothesis, Shapiro's step function point-source model may be applied as a first approximation. (The fossil karst provides a large pressurized water source, the pressure of which decreased very slowly.) We neglect changes in

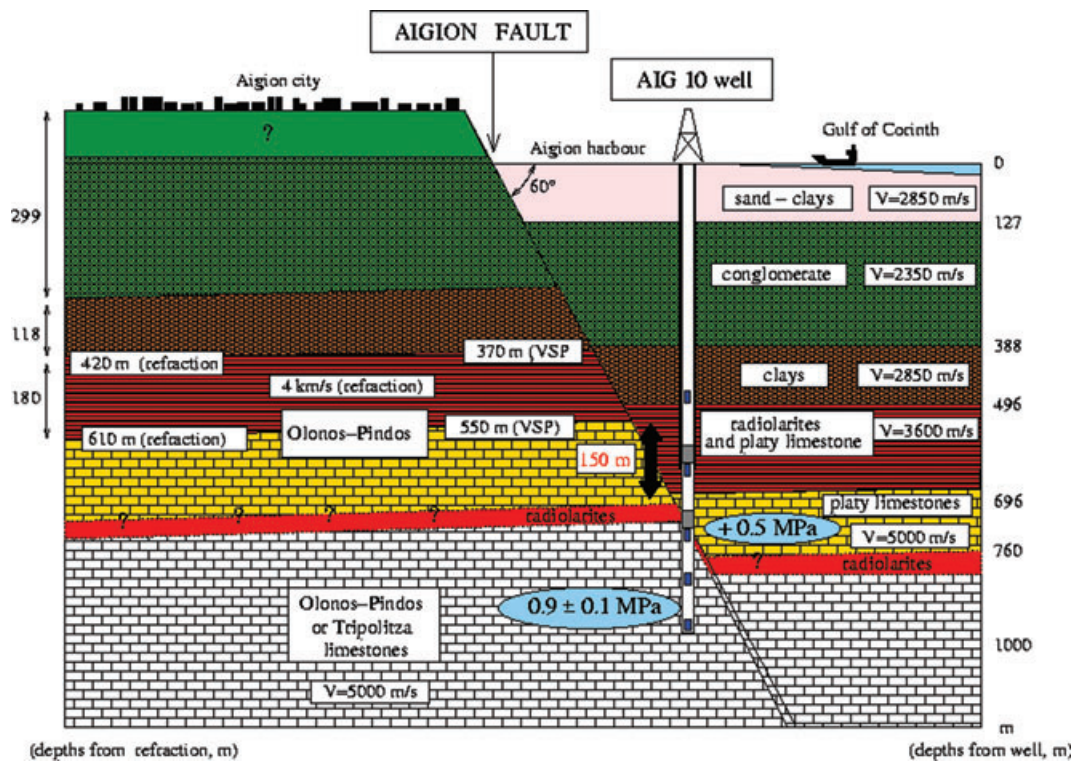


Figure 14. Schematic vertical cross-section, as established with the 1000 m deep AIG10 well (Cornet *et al.* 2004; Place *et al.* 2007). The figure outlines the two deep aquifers separated by the Aigion Fault (see the text).

hydraulic diffusivity within the cataclastic zone in the hanging wall and assume a more or less 2-D permeable structure (two thin permeable zones along the fault separated by an inner impervious clay film). Then Fig. 6 shows a linear increase of the distance between the diffusion front and the source, which results in a linear increase of the seismically activated area with time. This is consistent with a hydraulic diffusivity parallel to the fault system in the $10^4 \text{ cm}^2 \text{ s}^{-1}$ range, that is a value similar to those obtained by Talwani and Acree and Simpson *et al.* for water diffusion below dams down to 5 or 6 km, as well as by Parotidis *et al.* for the Eger Rift swarms.

This diffusion mechanism is proposed as a mechanism consistent with the overall swarm development. It is not meant to explain all seismic activity in the rift. In particular, a few events are observed ahead of the proposed diffusion front, especially at the beginning of the swarm activity. As mentioned earlier, their horizontal location is quite distant from the point taken as origin of the fluid migration. They are considered to be part of the continuous sparse rift seismic activity.

3.2.2 Sources of fluid overpressure and origin of the shallow dipping seismic zone

As already discussed, the seismic swarm development observed in 2003–2004 differs significantly from that observed during the August 2006–May 2007 period. For the latter one, we observed two independent domains of activity with simultaneously a downward and upward growth near the end of swarm activity. Thus, if fluid diffusion is the cause of this long-term activity, the pressure source seems to be generated by the deformation process itself.

In 2002, the seismic tomography conducted by Gautier *et al.* (2006) suggested an abundance of fluid within the seismically ac-

tivated region. But no clue was given as to where the fluids came from. Hydraulic data from AIG10 well demonstrate that the normal fault system constitutes a hydraulic barrier preventing flow from the south towards the north. Further the high mountain range (above 2000 m) to the south of the rift in the Peloponnese generates pressures above hydrostatic, hence resulting in downward flow directed more or less in the South–North direction given the rift orientation. This hydraulic potential may generate transient overpressures at depth through occasional rupturing of the hydraulic barriers constituted by the normal fault system because of the rift opening process.

But this topography is observed all along the 120 km length of the rift zone and no swarm activity is observed in the eastern section of the rift (see introduction). So an additional condition must prevail in the Aigion area for causing the observed activity. Some information with this respect is provided by the 2001 seismic crisis on the south shore (location accuracy better than 1 km, Lyon-Caen *et al.* 2004).

Following the same methodology as for the two seismic swarms already discussed, we identify a starting time and a starting location for the swarm. Then azimuthal plots of depth of events for various time windows outline the main geometric features of the swarm development (Fig. 15). These plots show that the seismic crisis starts initially at two different depths (around 5 km and around 9 km). But then the deep seismic activity migrates progressively upwards, while the shallow activity stops. Further, within the accuracy of the location procedure, the seismic crisis is found to be rather axisymmetrical, without large horizontal extension. Further it does not fit well with a south extension of the postulated shallow dipping decollement zone, but rather roots lower than 13 km (Fig. 5). The slow, localized, upward growth has the same duration characteristics as the previous ones so that we may assume it is fluid driven (mean growth velocity close to 1 m hr^{-1}). If indeed it is associated with

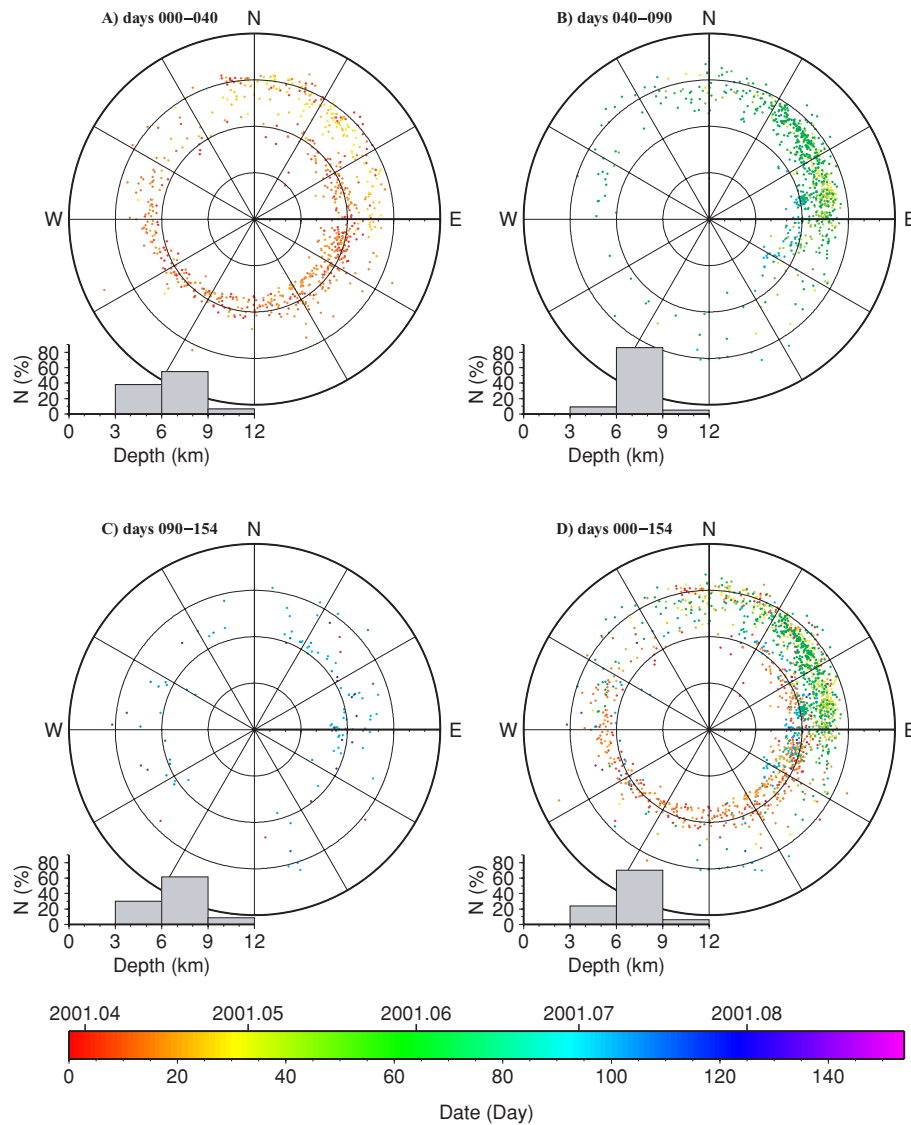


Figure 15. Azimuthal variation of depth, with time for the 2001 swarm activity. Although two centres of activity are observed when the swarm starts, only the deepest source remains active during the whole swarm duration. It starts in the northern direction around a 9 km depth and migrates progressively upwards to the South East where it reaches depths close to 5 km.

fluid migration, this implies an overpressure migrating upwards, not consistent with the downward regional flow identified during the 2003–2004 swarm activity. It may be associated with a deeper fluid source. Such a conclusion on upward fluid diffusion has also been reached by Pacchiani & Lyon-Caen (2009) with a much more refined procedure for the seismic events' location determination.

Hence, the three seismic swarms (2001, 2003–2004, 2006–2007) suggest non-steady pore pressure conditions within the seismogenic zone. The downgoing seismic propagation observed during the 2003–2004 seismic crisis requires a subhydrostatic pressure level within the seismogenic zone (overpressure smaller than a few MPa since it is topography driven), if it is associated with downward fluid diffusion. The 2001 seismic crisis suggests an upward migration of fluids of deep origin.

Existence of fluids of deep origin in the Aigion Fault cataclastic zone, as well as in the Mamousia Fault zone south of Aigion, has been documented (Baud *et al.* 2004; Pick & Marty 2008) from geochemical analysis of the fault gouge. Baud *et al.* provide evi-

dence of fluids coming from reservoirs where silicate dissolution was occurring. Given the uplift observed in the southern shore of the Corinth rift (Armijo *et al.* 1996; Rohais *et al.* 2007), the upward displacement of these samples cannot exceed 2–3 km, so upward flow through preferential channels is required for bringing fluids of deep origin (10 km range) at today's sampling depths. We may also mention that Koukouvelas & Papoulis (2009) have identified amorphous iron oxides within the outcropping fault zones, which they associate with fluid circulations originated at temperatures in the 100°C range. Given the low regional thermal gradient (lower than 20° km⁻¹, Doan & Cornet 2007) and the maximum possible uplift of this fault material (less than 3 km), this may be taken again as evidence of deeper fluids upflow.

Some evaluation of the transitory overpressure value that occurs within the seismogenic zone may be proposed from simple mechanical considerations. As already mentioned, Rietbrock *et al.* (1996) have demonstrated from multiplet analysis that slip occurs occasionally on planes with dip as shallow as 20° at a depth of

9.5 km. Given the rifting activity, it may be assumed that the maximum principal stress component is vertical. Then the pore pressure value required to induce slip along such 20° dipping plane is much larger than just subhydrostatic. It may be evaluated by assuming that fault stability is controlled by Byerlee's law [$\tau = \mu(\sigma_n - P)$ where τ and σ_n are, respectively, the shear and normal stress components supported by the fault, μ is the friction coefficient and P is the interstitial pore pressure]. With a 0.6 friction coefficient and a horizontal minimum principal stress equal to about half the principal vertical component (a feature quite standard for rifting conditions, Cornet *et al.* 2007) the pore pressure must reach 135 MPa to initiate slip at 8 km on a 20° dipping plane. Indeed, at 8 km depth the normal stress supported by planes dipping 20° in the minimum principal stress direction is 188 MPa whereas the shear stress is only 32 MPa, if we assume a 0.025 MPa m⁻¹ gradient for the vertical stress component. This 0.025 MPa m⁻¹ value is consistent with the local sedimentary rock density that is supposed to be present at least down to 4 km, leading to a minimum principal stress equal to about 100 MPa. Hence, this pressure value is about 35 MPa larger than the minimum principal stress at the same depth. It is also 55 MPa larger than the hydrostatic pressure associated with sea level. This shows that if slip episodes observed on the 20° dipping planes result from bursts of pressurized fluids, these outbursts can only be very temporary; otherwise, the overpressure would generate vertically oriented hydraulic fractures. Further, these pressure values cannot be associated with simple topographic effects. Hence, either they are generated by the deformation process itself or they are linked to occasional bursts of fluids from deeper origin. The 2006–2007 crisis is a strong support to the hypothesis of a dynamic origin for the fluid overpressure (i.e. pressure variation generated by the dynamic deformation process), but the 2001 crisis indicates that deep fluid sources are also occasionally active.

Following poro-elasticity theory (Wang 2000), the change in pore pressure ΔP within an undrained saturated elastic rock mass that supports an external change in the mean stress ΔS ($\Delta S = (\Delta\sigma_1 + \Delta\sigma_2 + \Delta\sigma_3)/3$) depends on the Skempton coefficient B ($\Delta P = B\Delta S$). B varies between 0.5 and 1 for saturated rocks but is close to 1 for saturated soils. Accordingly, the pore pressure variation to be expected from poro-elasticity, when the shear stress completely relaxed at 8 km depth is likely to be smaller than 30 MPa ($\Delta S = 33$ MPa if $\Delta\sigma_3 = 100$ and $\Delta\sigma_1 = \Delta\sigma_2 = 0$). This mechanism assumes that the vertical stress component, which is governed by gravity, remains unchanged and that the shear stress on the plane is completely released by the required increase of the minimum principal stress) for a Skempton coefficient equal to 0.9. Hence, a dynamic rise in pressure of the order of 35 MPa is not compatible with linear poro-elasticity but would require some kind of compaction of the rock-fault system to reach the required pressure variations. This non-elastic decrease of pore volume is likely to come from the mechanical behaviour of the faults themselves, following a somewhat similar mechanical behaviour to that of rock joints at shallower depth (e.g. Saeb & Amadei 1992; Gentier *et al.* 2000; Hopkins 2000; Grasselli & Egger 2003). Indeed, for rock joints under shallow conditions (small effective normal stress) it has been shown that first some volume increase occurs with shear displacement followed by a decrease in volume as displacement increases. Interestingly, a volume decrease associated with shearing is what is needed to generate rock failures inclined more than 45° to the maximum principal stress direction (Vardoulakis & Sulem 1995, Sulem 2007). A proper analysis along these lines would require some knowledge of the change in volume with deformation, but such data are not available yet.

It is concluded that, although a regional downgoing flux exists because of topography and the hydraulic properties of normal faults, seismicity on shallow dipping planes within the seismic zone cannot be related only to this downgoing flux. It requires high transitory pore pressure values that are possibly generated dynamically by the deformation process itself. In the long term, the pore pressure within the seismic zone cannot become larger than the minimum principal stress magnitude since larger values are released through hydraulic fracturing.

This simple model implies that the observed shallow dipping orientation of the seismic zone may correspond to a freshly formed shallow dipping fault zone that does not obey Coulomb theory but rather follow the principles of plasticity with coupled volumetric variation (Arthur *et al.* 1977; Vardoulakis 1980; Vardoulakis & Sulem 1995). However, reactivation of pre-existing structures through high pore pressure variations associated with percolation of fluids of deeper origin may also be a possible mechanism.

3.2.3 Geographical extent of the fluid controlled swarm activity

From the CRLnet results alone, the domain in which microseismicity occurs repeatedly seems fairly limited spatially. However, this apparent small size of the seismogenic volume might be attributed to the small surface extension of CRLnet and to poor event detection outside the network perimeter. To examine the limitations of CRLnet detection, we turn to results obtained with the National Observatory of Athens (NOA) catalogue. Indeed, the NOA network has been considerably improved over the years and provides today very satisfactory detection of events with magnitude larger than 2.5 all over Greece. Fig. 1b clearly shows that the swarm activity is restricted to the Aigion area.

The seismic crisis that occurred in 2007 April some 40 km to the NW of the CRL location has been investigated with a local 15-station network by Kiratzi *et al.* (2008). Events' location has been determined through accurate double difference technique. Seismic events occur down to depths close to 20 km, that is at much greater depths than those near Aigion. Hence, the Aigion shallow dipping seismic zone does not extend further to the NW outside the CRLnet perimeter. It remains fairly constrained within the rift zone and does not extend towards the Patras gulf, west of the Corinth Gulf.

We conclude that the shallow dipping seismic zone near Aigion does not correspond to a large-scale decollement zone but only to a local deformation process associated with occasional bursts of fluids of deeper origin. The high pore pressure conditions within the seismogenic zone can only be transient, given hydraulic fractures develop when pore pressure gets larger than the minimum principal stress magnitude.

We see no argument to stop the over 20 km long Heliki Fault (for its onshore section) at a depth of 7 or 8 km, given the absence of shallow dipping seismic activity in the rift around this location. For the Aigion Fault, an extension at least down to 9 km is suggested by the observed activity (Fig. 5).

4 DISCUSSION: RELATIONSHIP BETWEEN OUTCROPPING NORMAL FAULTS AND THE SHALLOW DIPPING SEISMOGENIC ZONE

We propose that localization of seismic swarm activity is a combination of occasional upflow of fluids of deeper origin and regional downgoing flux of meteoric water. These occasional fluid bursts

are consistent with geochemical investigation on material sampled within the cataclastic zone of local faults. Although the localization process is linked to the local deep fluid flux, it may lead to plastic deformation (at the scale of the zone of swarm activity) associated with an overall volume decrease that generates low dipping slip zones.

The origin of the deep upflowing fluids has not been established yet, but at least two candidates may be proposed for their reservoir. One possible source is the hypothetical decollement zone likely to exist at depth, between 15 and 20 km, according to the measured heat flux, for accommodating through the lower crust the Corinth Rift opening (more than 10 km N–S extension). Another possible source is the subducting plate that exists at a fairly shallow depth under the rift zone (Mc Kenzie 1972; Wortel & Spakman 2000) and that is known to generate large quantities of fluids. Given that the Moho is around 40 km locally (Sachpazi *et al.* 2007), the cold subducting plate may not be very deep near Aigion, given the proximity of the subduction west of Patras. With this respect, the occurrence of a seismic crisis some 50 km south of Aigion in 2008 February, about 1 month after a magnitude 6.2 earthquake occurred on 2008 January 6 at a depth of 72 km some 130 km southeast of Aigion (NOA catalogue), may not be simply fortuitous.

This proposed crustal fluid diffusion process may help shed some light on the relationship between the steeply dipping normal faults that outcrop in the southern shore of the rift and the shallow dipping seismogenic zone observed locally within this section of the rift zone. Whereas the Eastern branch of the Helike Fault (Fig. 2) has been the site of many historical magnitude 7 earthquakes, the western segment appears presently inactive in terms of microseismicity according to the NOA catalogue. This absence of seismic activity is consistent with de Martini *et al.*'s (2004) observation that the western branch of the Helike Fault has not been active over the last few thousand years. We propose as working hypothesis that a relationship exists between the proposed deep fluid circulation and the change in rift activity west of Aigion. Whereas the steeply dipping outcropping normal fault system reaches depths in the order of 10–15 km or more, a deep fluid circulation that started much after the rift extension has induced local relaxation of the deviatoric stress locally near Aigion. It has reduced the shear component of the stress field acting on the western branch of the Heliki Fault, enough to stop the local fault activity.

Interestingly, Cianetti *et al.* (2008) have proposed a new model for the displacement field described by Avalone *et al.* (2004) for the Aigion area. They note that the displacement field observed over the 11 yr of repeated surveys does not require a local detachment at 8 km but may be explained by a simple elasto-plastic model with only steeply dipping active faults. So clearly the surface displacement field over the last 11 yr is not a strong enough constraint for debating upon the existence of a decollement zone around 8 km.

We propose as a hypothetical mechanism that the upward fluid flux that occurs through deep structures not seen on ground surface (like the one identified on Fig. 10d) has released the stress field on the Western Helike Fault and is redistributing tectonic stresses to the northwest of the Aigion area. Only long-term monitoring of the seismic activity will validate this hypothesis.

5 CONCLUSION

Our analysis of the seismic activity in the Aigion area during the last 8 yr has shown that the shallow dipping active zone identified during previous short-term monitoring periods exhibits a fairly

complex structure. It combines both subvertical structures with diverse orientations and shallow dipping planes. The swarm activity supported by this complex structure is compatible with some fluid diffusion. Most of the fluid is provided by rain and snowfall on the high topography that borders the rift, as demonstrated by the downgoing seismic migration observed for the 2003–2004 seismic crisis. However, transitory high over-pressures are required to generate slips on low dipping planes. A plastic deformation mechanism associated with a volume decrease may be proposed for generating these shallow dipping surfaces. It will be explored further once a detailed understanding of both the fracture pattern and the volume variation with shear displacement for these fault zones is available.

However, the Corinth Rift is more than 120 km long and on both sides of the rift we observe mountains with elevation larger than 2000 m. Yet only near Aigion has a swarm activity been observed over the 40 yr of data provided by the NOA catalogue. We propose to associate the swarm activity with occasional up flow of fluid, as evidenced by the upward migration of the 2001 seismic crisis. Whether these fluids are originated in the deeper crust, possibly in a decollement zone through the lower crust, or whether they are associated with the 70 km deep subducting plate remains to be explored.

The observed seismic activity shows that the Aigion Fault roots down at least to 8 or 9 km. No argument has been found to stop the Heliki fault at the same depth. In contrast, observations from the recent seismic activity that occurred to the northeast of CRL have demonstrated that brittle behaviour with steeply dipping faults extends at least down to 20 km. Hence, it seems logical to consider that the 20 km long Heliki Fault roots down to similar depths.

We see no evidence for associating the seismic swarm activity in the Aigion area with a large-scale low dipping decollement zone of significance at the 100 km scale. Rather we conclude that the shallow dipping seismic activity is only local and results very likely from the circulation of fluids, only a small part of which has a fairly deep origin. This deep fluid source may be the cause for the recent absence of tectonic activity on the western Heliki Fault.

A deep borehole that would provide means to sample the circulating fluids and monitor the high frequency microseismic activity at depth would help to obtain the parameters required to validate such a model and better establish our proposition that, in the Corinth Rift near Aigion, the hydraulic diffusivity along the cataclastic zone of active, or recently activated, faults is in the range 10^3 – 10^4 cm² s⁻¹.

ACKNOWLEDGMENTS

We thank very sincerely A. Deschamps, Nikos Geremenis and Genevieve Pateau for their help in maintaining the system operational and for conducting the time corrections on the various stations. This work would not have been possible without the help of many helpers who conducted the arrival times picking. Discussions with Thymos Sockos have been very beneficial for better understanding the seismic activity in western Greece. The work was funded through the French Centre National Research Centre (CNRS) and the French Agence Nationale pour la Recherche (contract nb). The AIG10 well was drilled with support from the European Commission (contract nb EVR1-CT-2000-40005) and support from the International Continental Drilling Program. SB benefited from a post-doc fellowship from the EU supported AEGIS program (contract nb) and from support from Institut de Physique du Globe de Paris. Finally, we wish to thank very sincerely M. Cara, T.

Fisher, Y. Ben Zion and two anonymous reviewers who helped us to improve very significantly the original manuscript.

REFERENCES

- Armijo, R., Meyer, B., King, G.C.P., Rigo, A. & Papanastasiou, D., 1996. Quaternary evolution of the Corinth Rift and its implications for the late Cenozoic evolution of the Aegean, *Geophys. J. Int.*, **126**, 11–53.
- Arthur, J.R.F., Dunstan, T., Al-Ani, Q.A.J. & Assadi, A., 1977. Plastic deformation and failure in granular material, *Geotechnique*, **27**, 53–74.
- Avalonne, A. *et al.* 2004. Analysis of 11 years of deformation measured by GPS in the Corinth Rift area, *C.R. Geosci.*, **336**(4–5), 301–312.
- Baer, M. & Kradolfer, U., 1987. An automatic phase picker for local and teleseismic events, *Bull. seism. Soc. Am.*, **77**(4) 1437–1445.
- Baud, P. *et al.*, 2004. Circulation des fluides dans les systèmes de failles du Rift de Corinthe; Données structurales, pétrophysiques de porosité et de géochimie; rapport GDR " Corinth " (unpublished, <http://www.corinth-rift-lab.org>).
- Bell, R.E., McNeill, L.C., Bull, J.M. & Henstock, T.J., 2008. Evolution of the western Gulf of Corinth, *Bull. geol. Soc. Am.*, **120**(1/2), 156–178, doi:10.1130/B26212.1.
- Bell, M.L. & Nur, A., 1978. Strength changes due to reservoir-induced pore pressure and stresses and application to lake Oroville, *J. geophys. Res.*, **83**, 4469–4483.
- Bernard, P. *et al.*, 1997. The Ms = 6.2, June 15, 1995, Aigion earthquake (Greece); evidence for low angle normal faulting in the Corinth rift, *J. Seism.*, **1**, 131–150.
- Bernard, P. *et al.*, 2006. Seismicity, deformation and seismic hazard in the western rift of Corinth: new insights from the Corinth Rift Laboratory (CRL), *Tectonophysics*, **426**, 7–30.
- Briole, P. *et al.* 2000. Active deformation of the Corinth rift, Greece: results from repeated Global Positioning System surveys between 1990 and 1995, *J. geophys. Res.*, **105**, 25605–25625.
- Burton, P.W., Xu, Y., Qin, Ch., Tselentis, G. & Sokos, E., 2004. A catalogue of seismicity in Greece and the adjacent areas for the twentieth century, *Tectonophysics*, **390**, 117–127.
- Cianetti, S., Tinti, E., Giunchi, C. & Cocco, M., 2008. Modeling deformation rates in the Western Gulf of Corinth: rheological constraints, *Geophys. J. Int.*, **174**(2), 749–757.
- Cichowicz, A., 1993. An automatic S-phase picker, *Bull. seism. Soc. Am.*, **83**(1), 180–189.
- Cornet, F.H., 2000. Comments on “Large-scale *in situ* permeability tensor of rocks from induced microseismicity” by Shapiro, Audigane and Royer (1999), *Geophys. J. Int.*, **140**(b2), 465–469.
- Cornet, F.H., Berard, Th. & Bourouis, S., 2007. How close to failure is a natural granite rock mass at 5 km depth? *Int. J. Rock Mech. Min. Sci.*, **44**(1), 47–66.
- Cornet, F.H., Bernard, P. & Moretti, I., 2004a. The Corinth Rift Laboratory, *C.R. Geosci.*, **336**, 235–241.
- Cornet, F.H., Doan, M.L., Moretti, I. & Borm, G., 2004b. Drilling through the active Aigion Fault: the AIG10 well observatory, *C.R. Geosci.*, **336**, 395–406.
- Cornet, F.H. & Yin, J., 1995. Analysis of induced seismicity for stress field determination and pore pressure mapping, *Pure appl. Geophys.*, **145**(3/4), 677–700.
- Daniel, J.M., Moretti, I., Micarelli, L., Essautier-Chuyne, S. & Delle Piane, C., 2004. Macroscopic structural analysis of AIG10 well (Gulf of Corinth, Greece), *C.R. Geosci.*, **336**(4–5), 435–444.
- De Martini, P.M., Pantosti, D., Palyvos, N., Lemeille, F., McNeil, L. & Collier, R., 2004. Slip rates of the Aigion and Eliki Faults from uplifted marine terraces, Corinth Gulf, Greece, *C.R. Geosci.* **336**, 325–334.
- Doan, M.L. & Cornet, F.H., 2007a. Thermal anomaly near the Aigio fault, Greece, may be due to convection below the fault, *Geophys. Res. Lett.*, **34**, L06314, doi:10.1029/2006GRL028931.
- Doan, M.L. & Cornet, F.H., 2007b. Small pressure drop near a fault induced by small teleseismic waves, *Earth planet. Sci. Lett.*, **258**, 207–218.
- Earle, P.I.S. & Shearer, P.M., 1994. Characterization of global seismograms using an automatic-picking algorithm, *Bull. seism. Soc. Am.*, **84**(2), 366–376.
- Fehler, M., House, L. & Kaieda, H., 1987. Determining planes along which earthquake occur: method and application to earthquakes accompanying hydraulic fracturing, *J. geophys. Res.*, **92**(B9), 9407–9414.
- Gautier, S., Latorre D., Virieux J., Deschamps A., Skarpos C., Sotiriou A., Serpetsidaki A. & Tselentis A., 2006. A new passive tomography of the Aigion area (Gulf of Corinth, Greece) from the 2002 dataset, *Pure appl. Geophys.*, **163**(2), 431–453, doi:10.1007/s00024-005-0033-7.
- Gentier, S., Riss, J., Archambault, G., Flamand, R. & Hopkins, D., 2000. Influence of fracture geometry on shear behaviour, *Int. J. Rock Mech. Min. Sci.*, **37**(1–2), 161–174.
- Giurgea, V., Rettenmaier, D., Pizzino, L., Unkel, I., Hötzel, H., Förster, A. & Quatrocchi, F., 2004. Preliminary hydrogeological interpretation of the Aigion area from the AIG10 borehole data, *C.R. Geosci.*, **336**, 467–476.
- Grasselli, G. & Egger, P., 2003. Constitutive law for the shear strength of rock joints based on three-dimensional surface parameters, *Int. J. Rock Mech. Min. Sci.*, **40**, 25–40.
- Gupta, H.K., 1983. Induced seismicity hazard mitigation through water level manipulation at Koyna, India: a suggestion, *Bull. seism. Soc. Am.*, **73**, 679–682.
- Hainzl, S. & Fischer, T., 2002. Indications for a successively triggered rupture growth underlying the 2000 earthquake swarm in Vogtland /NW Bohemia, *J. geophys. Res.*, **107**, ESE 5-1, 5-9, B12, doi:10.1029/2002JB001865.
- Hainzl, S. & Ogata Y., 2005. Detecting fluid signals in seismicity data through statistical modelling, *J. geophys. Res.*, **110**, B05S07, doi:10.1029/2004JB003247.
- Hatzfeld, D., Karakostas, V., Ziazia, M., Kassaras, I., Papadimitriou, P., Makropoulos, K., Voulgaris, N. & Papaioannou, C., 2000. Microseismicity and faulting geometry in the Gulf of Corinth (Greece), *Geophys. J. Int.*, **141**, 438–446.
- Healy, J.H., Rubey, W.W., Griggs, D.T. & Raleigh, C.B., 1968. The Denver earthquakes, *Science*, **161**, 1301–1310.
- Hopkins, D.L., 2000. The implications of joint deformation in analyzing the properties and behavior of fractured rock masses, underground excavations and faults, *Int. J. Rock Mech. Min. Sci.*, **37**, 175–202.
- Hubert, A., King, G., Armijo, R., Meyer, B. & Papanastasiou, D., 1996. Fault re-activation, stress interaction and rupture propagation of the 1981 Corinth earthquake sequence, *Earth Planet. Sci. Lett.*, **142**, 573–585.
- Jolivet, L., Rimmelé, G., Oberhänsli, R., Goffé, B. & Candan, O., 2004. Correlation of syn-orogenic tectonic and metamorphic events in the Cyclades, the Lycian Nappes and the Menderes massif, geodynamic implications, *Bull. Geol. Soc. France*, **175**, 217–238.
- Kanamori, H. & Anderson, D.L., 1975. Theoretical basis of some empirical relations in seismology, *Bull. seism. Soc. Am.*, **65**(5), 1073–1095.
- Kiratzis, A. *et al.* 2008. The April 2007 earthquake swarm near Lake Trichionis and implication for active tectonics in western Greece, *Tectonophysics*, **452**, 51–65.
- Koukouvelas, I.K. & Papoulis, D., 2009. Fluid involvement in the Helike normal fault, Gulf of Corinth Greece, *J. Struct. Geol.* **31**, 237–250.
- Lyon-Caen, H., Papadimitriou, P., Deschamps, A., Bernard, P., Makropoulos, K., Pacchiani, F. & Patau, G., 2004. First results of the CRLN seismic network in the western Corinth Rift: evidence for old fault reactivation, *C.R. Geosci.*, **336**(4–5), 343–353.
- Makropoulos, K.C., Drakopoulos, J.K. & Latousakis, J.B., 1989. A revised and extended earthquake catalogue for Greece since 1900, *Geophys. J. Int.* **98**, 391–394.
- McNeil, L.C., Cotterill, C.J., Henstock, T.J., Bull, J.M., Stafatos, A., Collier, R.E.L., Papatheoderou, G., Ferentinos, G. & Hicks, S.E., 2005. Active faulting within the offshore western Gulf of Corinth, Greece: Implication tops models of continental rift deformation, *Geology*, **33**, 241–244.
- Main, I., 1996. Statistical Physics, Seismogenesis, and seismic hazard, *Rev. Geophys.*, **34**(4), 433–462.

- Mc Kenzie, D., 1972. Active tectonics of the Mediterranean region, *Geophys. J. R. astr. Soc.*, **30**, 109–185.
- National Observatory of Athens, National Institute of Geodynamics, *On-line Bulletin*, www.geib.noa.gr/service/cat.html, 2007.
- Pacchiani, F. & Lyon-Caen, H., 2009. Relocation and spatio-temporal evolution of the 2001 Agios Ioannis earthquake swarm (Corinth rift, Greece), *Geophys. J. Int.*, submitted.
- Parotidis, M., Rothert, E. & Shapiro, S.A., 2003. A possible triggering mechanism for the earthquake swarms 2000 in Vgtand/NW-Bohemia, central Europe, *Geophys. Res. Lett.*, **30**(20), 2075, doi:10.1029/2003GL018110.
- Pearson, C., 1981. The relationship between microseismicity and high pore pressure during hydraulic stimulation experiments in low permeability granitic rocks, *J. geophys. Res.*, **86**(B9), 7855–7864.
- Pick, R. & Marty, B., 2008. Helium isotopic signature of modern and fossil fluids associated with the Corinth rift fault zone (Greece): implication for fault connectivity in the lower crust, *Chem. Geol.*, in press.
- Place, J., Naville, C. & Moretti, I., 2007. Fault throw determination using 4 component VSP: Aigion Fault (Greece) case study, *Tectonophysics*, **440**, 141–158.
- Rettenmaier, D., Giurgea, V., Hötzl, H., Förster, A., 2004. The AIG10 drilling project (Aigion, Greece); interpretation of the litho-log in the context of regional geology and tectonics, *C.R. Geosci.*, **336**(4–5), 415–424.
- Rietbrock, A., Tiberi, C., Scherbaum, F. & Lyon-Caen, H., 1996. Seismic slip on a low angle normal fault in the Gulf of Corinth: evidence from high-resolution cluster analysis of microearthquakes, *Geophys. Res. Lett.*, **23**(14), 1817–1820.
- Rigo, A., Lyon-Caen, H., Armijo, R., Deschamps, A., Hatzfeld, D., Makropoulos, K., Papadimitriou, P. & Kasaras, I., 1996. A microseismic study in the western part of the Gulf of Corinth (Greece): implication for large-scale normal faulting mechanisms, *Geophys. J. Int.*, **126**, 663–688.
- Rohais, S., Eschard, R., Ford, M., Guillocheau, F. & Moretti, I., 2007. Stratigraphic architecture of the Plio-Pleistocene infill of the Corinth Rift: implications for its structural evolution, *Tectonophysics*, **440**, 5–28.
- Sachpazzi, M., Galvé, A., Laigle, M., Hirn, A., Sokos, E., Serpetsidaki, A., Pi Alperin, J.M., Zelt, B. & Taylor, B., 2007. *Tectonophysics*, **440**, 53–65.
- Saeb, S. & Amadei, B., 1992. Modelling rock joints under shear and normal loading, *Int. J. Rock Mech. Min. Sci.*, **29**, 267–278.
- Shapiro, S.A., Huenges, E. & Borm, G., 1997. Estimating the crust permeability from fluid-injection-induced seismic emission at the KTB site, *Geophys. J. Int.*, **131**, F15–F18.
- Simpson, D.W., Leith, W.S. & Scholtz, C.H., 1988. Two types of reservoir-induced seismicity, *Bull. seism. Soc. Am.*, **78**(6), 2025–2040.
- Song, I., Elphick, S.C., Odling, N., Main, I.G. & Ngwenya, B.T., 2004. Hydromechanical behaviour of the fined grained calcilitite and fault gouge from the Aigion Fault Zone, *C.R. Geosc.*, **336**(4–5), 445–454.
- Sulem, J., 2007. Stress orientation evaluated from strain localisation analysis in Aigion Fault, *Tectonophysics*, **442**, 3–13.
- Sulem Vardoulakis, J.I., Ouffroukh, H., Boulon, M. & Hans, J., 2004. Experimental characterization of the thermo-poro-mechanical properties of the Aegion Fault gouge, *C.R. Geosci.*, **336**(4–5), 455–465.
- Talwani, P. & Acree, S., 1984. Pore pressure diffusion and the mechanism of Reservoir-induced seismicity, *Pure appl. Geophys.*, **122**, 947–965.
- Vardoulakis, I., 1980. Shear band inclination and shear modulus of sand in biaxial tests, *Int. J. Numer. Anal. Meth. Geomech.*, **4**, 3–119.
- Vardoulakis, I. & Sulem, J., 1995. *Bifurcation Analysis in Geomechanics*, Chapman & Hall.
- Vardoulakis, I. & Sulem, J., 1995. Bifurcation in Geomechanics 459 p, Blackie Academic and Professionals, Glasgow, U.K.
- Wang, H.F., 2000. *Theory of Linear Poroelasticity*, Princeton University Press, Princeton, NJ.
- Wortel, M.J.R. & Spakman, W., 2000. Subduction and slab detachment in the Mediterranean-Carpathian Region, *Science*, **290**(5498), 1910–1917.